Comparison of the Structures and Wetting Properties of Self-Assembled Monolayers of *n*-Alkanethiols on the Coinage Metal Surfaces, Cu, Ag, Au[1]

Paul E. Laibinis,[†,2] George M. Whitesides,*[,†] David L. Allara,*[,‡] Yu-Tai Tao,[‡,§] Atul N. Parikh,[‡] and Ralph G. Nuzzo*[,#]

Contribution from the Department of Chemistry, Harvard University, Cambridge, Massachusetts 02138, Departments of Materials Science and Chemistry, Pennsylvania State University, University Park, Pennsylvania 16802, Departments of Materials Science and Chemistry, University of Illinois at Urbana—Champaign, Urbana, Illinois 61801, and AT&T Bell Laboratories, Murray Hill, New Jersey 07974. *Received January 14, 1991*

Abstract: Long-chain alkanethiols, $HS(CH_2)_nCH_3$, adsorb from solution onto the surfaces of gold, silver, and copper and form monolayers. Reflection infrared spectroscopy indicates that monolayers on silver and on copper (when carefully prepared) have the chains in well-defined molecular orientations and in crystalline-like phase states, as has been observed on gold. Monolayers on silver are structurally related to those formed by adsorption on gold, but different in details of orientation. The monolayers formed on copper are structurally more complex and show a pronounced sensitivity to the details of the sample preparation. Quantitative analysis of the IR data using numerical simulations based on an average single chain model suggests that the alkyl chains in monolayers on silver are all-trans zig-zag and canted by ~12° from the normal to the surface. The analysis also suggests a twist of the plane containing the carbon backbone of ~45° from the plane defined by the tilt and surface normal vectors. For comparison, the monolayers that form on adsorption of alkanethiols on gold surfaces, as judged by their vibrational spectra, are also trans zig-zag extended but, when interpreted in the context of the same single chain model, have a cant angle of ~27° and a twist of the plane of the carbon backbone of ~53°. The monolayers formed on copper (when they are obtained in high quality) exhibit infrared spectra effectively indistinguishable from those on silver and thus appear to have the same structure. Films on copper are also commonly obtained that are structurally ill-defined and appear to contain significant densities of gauche conformations. These spectroscopically based interpretations are compatible with inferences from wetting and XPS measurements. The structure of the substrate–sulfur interface appears to control molecular orientations of the alkyl groups in these films. An improved structural model, incorporating a two-chain unit cell and allowing for the temperature-dependent population of gauche conformations, is presented and applied to the specific case of the structures formed on gold.

Introduction

This paper describes the preparation and characterization of self-assembled monolayers (SAMs) formed by the chemisorption of alkanethiols ($HS(CH_2)_nR$) on surfaces of copper and silver. Both of these metal surfaces are highly active in the chemisorption of organosulfur compounds.[3-6] They offer an excellent opportunity to study the influences of the substrate in defining and controlling the order of self-assembled monolayer films. A central objective of this study was to compare the structures of the monolayers formed on silver and copper with those formed by chemisorption of alkanethiols on gold.[7-11] The molecular orientation and ordering of long-chain alkyl thiolate monolayers on gold reflects the epitaxial bonding of the sulfur atoms (or, perhaps more precisely, of gold thiolates) to the surface lattice plane. For long-chain alkyl disulfides and thiols chemisorbed on Au(111) (the preferred crystallographic texture of typical polycrystalline samples), electron diffraction (TEM and LEED)[10] has established that the sulfur atoms in the adsorbates form $(\sqrt{3} \times \sqrt{3})R30°$ overlayers. This epitaxial overlayer results in an interchain spacing of 4.99 Å and is well suited to the formation of close-packed, and therefore ordered, organic surface phases when the alkyl chain is long ($n \geq 15$) and the R group roughly commensurate in size with the polymethylene chain.[11,12] Several recent studies discuss these issues.[7-13]

Copper, silver, and gold have nearest neighbor spacings in the (111) plane of 2.56 Å, 2.89 Å, and 2.88 Å, respectively.[14] If structures form on copper and silver that are analogous to those on gold (i.e., $(\sqrt{3} \times \sqrt{3})R30°$), we expect the molecular orientations of the chains to differ significantly since the average chain density on copper would have to be considerably higher than on gold or silver (~17.03 Å²/chain on copper versus 21.75 Å²/chain on silver and 21.62 Å²/chain on gold). We would expect, given

[†] Harvard University.
[‡] Pennsylvania State University.
[§] Permanent Address: Institute of Chemistry, Academia Sinica, Taipei, Taiwan, ROC.
[#] AT&T Bell Laboratories; correspondence should be addressed to Department of Materials Science and Engineering, University of Illinois at Urbana-Champaign, Urbana, IL 61801.

(1) This highly collaborative work was supported by a variety of sources. G.M.W. acknowledges support from the Office of Naval Research, the Defense Advanced Research Projects Agency (DARPA), and the National Science Foundation (Grant CHE-88-12709). The XPS spectrometer was obtained through the DARPA University Research Initiative and maintained in the Harvard Materials Research Laboratory. D.L.A. and A.N.P. acknowledge support in part from the National Science Foundation (Grant DMR-9001270).

(2) Shell Foundation Pre-doctoral Fellow, 1987–88.

(3) Seymour, D. L.; Bao, S.; McConville, C. F.; Crapper, M. D.; Woodruff, D. P.; Jones, R. G. *Surf. Sci.* **1987**, *189–190*, 529–534. Anderson, S. E.; Nyberg, G. L. *J. Electron Spectrosc. Relat. Phenom.* **1990**, *52*, 735–746.
(4) Sandroff, C. J.; Herschbach, D. R. *J. Phys. Chem.* **1982**, *86*, 3277–3279.
(5) Sandroff, C. J.; Garoff, S.; Leung, K. P. *Chem. Phys. Lett.* **1983**, *96*, 547–551. Joo, T. H.; Kim, K.; Kim, M. S. *J. Phys. Chem.* **1986**, *90*, 5816–5819. Sobocinski, R. L.; Bryant, M. A.; Pemberton, J. E. *J. Am. Chem. Soc.* **1990**, *112*, 6177–6183.
(6) Kwon, C. K.; Kim, K.; Kim, M. S.; Lee, S. B. *Bull. Korean Chem. Soc.* **1989**, *10*, 254–258.
(7) Nuzzo, R. G.; Allara, D. L. *J. Am. Chem. Soc.* **1983**, *105*, 4481–4483.
(8) Bain, C. D.; Troughton, E. B.; Tao, Y.-T.; Evall, J.; Whitesides, G. M.; Nuzzo, R. G. *J. Am. Chem. Soc.* **1989**, *111*, 321–335.
(9) Porter, M. D.; Bright, T. B.; Allara, D. L.; Chidsey, C. E. D. *J. Am. Chem. Soc.* **1987**, *109*, 3559–3568.
(10) TEM: Strong, L.; Whitesides, G. M. *Langmuir* **1988**, *4*, 546–558. LEED: Dubois, L. H.; Nuzzo, R. G. Unpublished results.
(11) Chidsey, C. E. D.; Liu, G.-Y.; Rowntree, P.; Scoles, G. *J. Chem. Phys.* **1989**, *91*, 4421–4423. Camillone, N., III; Chidsey, C. E. D.; Liu, G.-Y.; Putvinski, T. M.; Scoles, G. *J. Chem. Phys.* **1991**, *94*, 8493–8502.
(12) Nuzzo, R. G.; Dubois, L. H.; Allara, D. L. *J. Am. Chem. Soc.* **1990**, *112*, 558–564.
(13) Whitesides, G. M.; Laibinis, P. E. *Langmuir* **1990**, *6*, 87–96. Bain, C. D.; Whitesides, G. M. *Angew. Chem., Int. Ed. Engl.* **1989**, *101*, 522–528.
(14) Kittel, C. *Solid State Physics*, 5th ed.; Wiley: New York, 1976; p 32.

0002-7863/91/1513-7152$02.50/0

this constraint, that the chains on copper would be aligned closer to the surface normal direction than those on silver or gold. The interchain spacing in the orthorhombic form of polyethylene yields an average chain density in the *ab* plane of ~18.27 Å²/chain.[15] The epitaxial bonding of alkyl thiolates in a $(\sqrt{3} \times \sqrt{3})R30°$ overlayer on copper therefore may be precluded by the steric packing constraints imposed by the chains. Silver and gold, on the other hand, have very similar lattice constants, and we expect the monolayers formed on them to have similar structures *in the absence of other perturbations.*

The studies described here demonstrate that the structures formed by similar adsorbates on polycrystalline copper, silver, and gold surfaces with a preferred (111) texture are related but different. The structural characteristics of monolayers formed on copper are extremely sensitive to the history of the samples and the details of the experimental techniques used in their preparations. The best films we have obtained on copper were comprised of closest packed chains that contained few gauche conformations. The poorer quality films contained significant concentrations of gauche conformations. The monolayers obtained on silver are highly organized and contain only low concentrations of gauche conformations. The molecular orientations deduced from the data are compatible with surface phases for alkanethiolates on silver and copper that are close-packed and have significantly shorter interchain spacings than that found on gold.

We present evidence, both from our studies and from the literature, that the differences in the structures of the monolayers formed on copper, silver, and gold reflect the differences in the reactivity of the surface of the metal, particularly its susceptibility to oxidation on exposure to laboratory air. The surfaces of copper oxidize rapidly[16] (and may also adsorb other environmental contaminants) during preparation of the sample. Silver also oxidizes on exposure to the laboratory atmosphere, but oxidation is substantially less extensive than for copper; under ambient conditions, one or two monolayers of silver oxide form on the silver surface.[17] The adsorption of alkanethiols on silver is complex and involves, we believe, some combination of reduction of Ag(I) to Ag(0), direct conversion of Ag(I) surface oxides to Ag(I) thiolates, and formation of an ionic surface phase in which silver atoms have been removed from their equilibrium lattice positions. We use precedents established by LEED studies to derive this model and to rationalize the orientations determined by infrared spectroscopy. The data also suggest that, on prolonged exposure to the adsorbate solution, the surface becomes extensively sulfided, presumably forming a thin interfacial layer of Ag_2S.[18] Gold does not oxidize under ambient conditions, and the mechanism of conversion of alkanethiols to gold(I) alkanethiolates has still not been established unequivocally.[19] The high activity of silver and copper to oxygen and to thiols established the assembly procedures we used for reproducible formation of high-quality monolayers. The length of exposure of the unfunctionalized surface to the atmosphere, the solubility of the adsorbate in the contacting solvent, and the time of exposure to the solution of alkanethiol—variables that are generally unimportant in the reproducible assembly of alkanethiols on gold—were very important on copper and moderately important on silver.

Results

Phenomenological Differences in the Assembly of Alkanethiols on Copper, Silver, and Gold. The assembly of high-quality alkanethiolate monolayers on gold is straightforward.[7-13,20,21] Silver and copper, in contrast, readily form oxides that adsorb polar contaminants. We suspect the surfaces of these metals become rougher and more heterogeneous with extended exposure to air. Oxidized surfaces of copper and silver are active to the chemisorption of alkanethiols; the monolayers formed differ, however, in structure and properties from those formed on less oxidized surfaces. The differences can be rationalized by hypothesizing that the monolayer has formed on a roughened metal/metal oxide interphase and may itself be structurally heterogeneous. The most reproducible and highest quality monolayers we have obtained on silver and copper resulted from procedures in which freshly evaporated films were transferred rapidly under inert atmospheres into adsorbate-containing solutions. Manipulation of unfunctionalized substrates in air, prior to derivatization, resulted in monolayers that exhibited larger hystereses in contact angles and appeared less crystalline by IR and compositionally less homogeneous by XPS.

We begin by commenting on the influence of the solvent on the monolayers formed from thiols dissolved in them.[22] We exposed slides of the three metals to 1 mM octadecanethiol solutions in a range of solvents (isooctane, chloroform, tetrahydrofuran, acetonitrile, acetone, and ethanol) for 2 to 4 h and measured the advancing and receding contact angles (θ_a and θ_r) of water and hexadecane (HD). The slides were transferred from the evaporator into solutions under flowing argon to minimize effects due to laboratory exposure. In general, we observed no significant differences in wetting (or hysteresis = $\cos\theta_r - \cos\theta_a$) that could be attributed to the solvent (wetting data are available in the supplementary material). Monolayers formed on copper exhibited greater hysteresis than those formed on gold or silver. The wettabilities of the monolayers formed on all three metals are similar to those reported for oriented alkyl monolayers on other substrates.[8,23-26] XPS data also demonstrate that the solvents listed above are unreactive toward the substrates under these conditions.

Copper and silver did prove to be more reactive to alkanethiols and more sensitive to attributes of the alkanethiol than gold. For example, reaction of short alkanethiols ($n \leq 3$) with the copper and silver surfaces often resulted in surfaces that appeared discolored and sometimes visibly pitted; continued exposure seemed to result in dissolution of the metal. With increased chain length, the reproducibility of formation of high-quality monolayers (as determined by wetting and XPS) increased dramatically.[27] With longer alkanethiols, the solubility of the adsorbate became important. Docosanethiol, which is soluble in ethanol with warming, often formed multilayered structures on copper when adsorbed from ethanol;[28] adsorption from isooctane reproducibly resulted in monolayer films.

Adsorption times of 2 to 12 h yielded monolayers with the greatest reproducibility; we used these intervals in the studies

(15) Bunn, C. W. *Trans. Faraday Soc.* **1939**, *35*, 482-491. Walter, E. R.; Reding, F. P. *J. Polym. Sci.* **1956**, *21*, 561-562.
(16) Lawless, K. R.; Gwathmey, A. T. *Acta Metall.* **1956**, *4*, 153-163.
(17) Rovida, G.; Pratesi, F.; Maglietta, M.; Ferroni, E. *Surf. Sci.* **1974**, *43*, 230-256. Rovida, G.; Pratesi, F. *Surf. Sci.* **1975**, *52*, 542-555. Englehardt, H. A.; Menzel, D. *Surf. Sci.* **1976**, *57*, 591-618 and references cited therein.
(18) The promotion of silver tarnishing by sulfur-containing compounds is well known. See, for example: Graedel, T. E.; Franey, J. P.; Gaultieri, G. J.; Kammlott, K. W.; Malm, D. L. *Corros. Sci.* **1985**, *25*, 1163-1180 and references cited therein.
(19) An oxidizing coreactant is not required: Dubois, L. H.; Nuzzo, R. G. Unpublished results.
(20) Bain, C. D.; Evall, J.; Whitesides, G. M. *J. Am. Chem. Soc.* **1989**, *111*, 7155-7164.
(21) Laibinis, P. E.; Hickman, J. J.; Wrighton, M. S.; Whitesides, G. M. *Science (Washington, DC)* **1989**, *245*, 845-847.
(22) The nature of the solvent used has been shown to affect the wettability of monolayers on gold derived from polar-terminated alkanethiols.[20] Extension of these systems to the generation of high-energy organic interfaces requires the assembly be compatible with polar, hydrogen-bonding solvents.
(23) Cohen, S. R.; Naaman, R.; Sagiv, J. *J. Phys. Chem.* **1986**, *90*, 3054-3056. Tillman, N.; Ulman, A.; Schildkraut, J. S.; Penner, T. C. *J. Am. Chem. Soc.* **1988**, *110*, 6136-6144. Wasserman, S. R.; Tao, Y.-T.; Whitesides, G. M. *Langmuir* **1989**, *5*, 1074-1087.
(24) Allara, D. L.; Nuzzo, R. G. *Langmuir* **1985**, *1*, 45-52.
(25) Chen, S. H.; Frank, C. W. *Langmuir* **1989**, *5*, 978-987.
(26) Troughton, E. B.; Bain, C. D.; Whitesides, G. M.; Nuzzo, R. G.; Allara, D. L.; Porter, M. D. *Langmuir* **1988**, *4*, 365-385.
(27) We believe that the alkane provides a passivating layer that slows corrosion of the copper and silver by the alkanethiols.
(28) The films formed from ethanol were extremely hydrophobic ($\theta_a^{H_2O} \approx 130°$), exhibited large hystereses, and were wet by hexadecane. We believe the wetting behavior to be consistent with formation of a porous, precipitated layer of alkyl thiol and/or disulfide. The films prepared in ethanol could be grown to the point of being visible and were robust to washing with ethanol; washing with hexanes resulted in dissolution but did not reveal an underlying monolayer film that was not wet by hexadecane. This problem was more acute on copper than on silver; it was also more prevalent at lower temperatures.

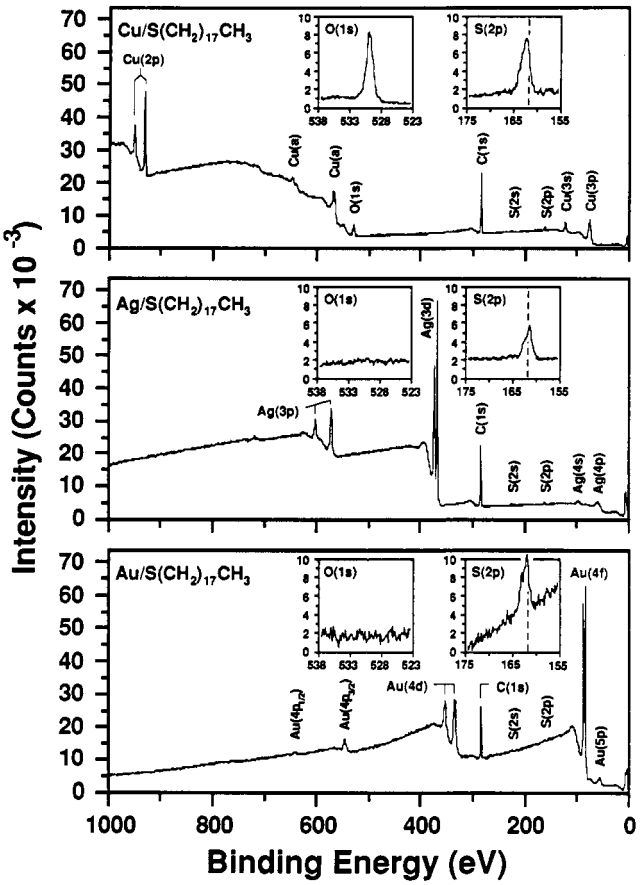

Figure 1. XPS spectra of monolayers of octadecanethiol adsorbed on surfaces of copper, silver, and gold. High-resolution spectra of the O(1s) and S(2p) regions are presented in the insets and were referenced to C(1s) = 284.80 eV. The dashed lines are provided for comparison of the S(2p) spectra. The binding energies of S(2s) and $S(2p_{3/2})$ are given in Table I and compared with values obtained for docosanethiol.

whose descriptions follow. Greater reproducibility on silver and copper was obtained with longer *n*-alkanethiols when isooctane was used as the solvent owing to the increased solubility of the adsorbates studied in this solvent. Adsorptions onto copper surfaces were conducted from isooctane; adsorptions onto the surfaces of gold and silver used ethanol or isooctane. No structural differences *in the high-quality films* were observed on any metal that could be assigned to solvent; those differences that were observed, we attribute to the solubility of the adsorbate or to surface roughening.

As indicated, to minimize the effects of oxidation and contamination, we transferred the slides of copper and silver to nitrogen-purged solutions of the thiols under a flowing stream of argon immediately following the evaporation of the metal. Occasionally, this procedure did not result in formation of high-quality monolayers on copper. We believe, however, that instrumental parameters for the evaporator (background pressure during the deposition, argon flow rate, etc.) were responsible for these failures and stress the importance of excluding oxygen (to the extent possible) to form monolayers on copper of the quality we have characterized. Silver could be exposed to air, to a limited degree, without exhibiting the catastrophic failures found for copper. We decided, based on the insensitivity of gold to the atmosphere, that anaerobic transfer was unnecessary; the films were manipulated in air and transferred to solution within 1 h of evaporation.

The monolayers formed on all three metals are stable to physical manipulation and washing with polar solvents. The monolayers on copper and silver do, however, exhibit only limited stability to air (changes are observed after ~1 week of exposure),[29] but could be routinely manipulated in ways previously detailed for alkanethiolate monolayers assembled on gold.[8]

(29) Laibinis, P. E.; Whitesides, G. M. Unpublished results.

Table I. Wetting Properties and XPS Binding Energies of Monolayers of Octadecanethiol Adsorbed on Copper, Silver, and Gold and of Related Materials

	wetting (θ_a, θ_r),[a]		XPS binding energies (eV)[b]	
	H_2O	HD	$S(2p_{3/2})$	S(2s)
$HSC_{22}H_{45}$	NA	NA	163.6[c]	217.9
$Au^{I}SC_{16}H_{37}$	NA	NA	162.6[d]	
$Cu/SC_{18}H_{37}$	120, 103	48, 32	162.1	226.2
$Ag/SC_{18}H_{37}$	116, 103	50, 40	162.3	225.7
$Au/SC_{18}H_{37}$	115, 105	48, 36	161.9	226.4
$Ag{\cdot}Ag_2O + HO_3SC_{16}H_{33}$	96, 61	<15, –[e]	167.4	231.6

[a] HD = hexadecane. NA = not applicable. [b] Binding energies for all samples were referenced to C(1s) = 284.80 eV. [c] For comparison, ref 31 reports a value of 163.3 eV (referenced to C(1s) = 284.7 eV). [d] Reference 31. Gold(I) thiolates are polymeric species; caution should be exercised in comparing their spectral properties directly with those obtained on monolayers. [e] A dash indicates a receding constant angle for a contacting liquid that could not be removed from the surface; $\theta_r \cong 0°$.

Scanning Electron Microscopy (SEM). The morphologies of the various substrates after exposure to octadecanethiol were examined by scanning electron microscopy. The surfaces of the three substrates, when prepared under comparable conditions, are similar. The copper and silver samples appear to have the same "rolling hills" texture that has been described for films of gold evaporated onto silicon wafers.[8] The amount of roughening due to oxidation or reaction of the copper or silver surfaces with alkanethiols does not appear to induce any perceptible morphological changes at the level of resolution of SEM (~200–500 Å).

X-ray Photoelectron Spectroscopy (XPS). Representative XPS spectra of monolayers obtained by reaction of octadecanethiol on copper, silver, and gold are given in Figure 1. The most significant feature in these spectra is the content of impurities of the films, as inferred from the intensities of peaks in the O(1s) core level region (binding energy ~535 eV). Clearly, the alkanethiolate monolayer on copper is adsorbed on an interphase containing a significant quantity of oxide. Treatment of highly oxidized copper surfaces with thiols results, as judged by XPS, in a decrease in the content of oxygen and a complete loss of peaks due to Cu(II).[29] The residual oxygen content of the copper interface remains high, however, suggesting that only a partial displacement of near-surface oxygen atoms occurs on exposure to the adsorbate. The residual oxide content of the monolayer on silver is very low, perhaps of the order of a few percent of a monolayer. The adsorption of thiol on silver thus must either reverse any oxidation of the substrate that has occurred or displace a significant fraction of oxygen species generated by it. Further discussion of this point will be deferred to the Discussion section. On gold, the oxygen content of the film is below the detection limit of XPS. The character of the sulfur–surface bond is indicated by the high-resolution core level data in the S(2p) region (Table I and Figure 1). The binding energies measured for the $2p_{3/2}$ core level on copper, silver, and gold (162.1, 162.3, and 161.9 eV, respectively) are all well within the range expected for a surface thiolate (RS–M or RS^-M^+) species.[30,31] These values would implicate a formal dissociative adsorption of the S–H bond on the metal on all three substrates (eq 1).[4,6,31]

$$RSH + M(0) \rightarrow RS\text{-}M(I) + \text{“}\tfrac{1}{2}H_2\text{”} \quad (1a)$$

or

$$RSH + M(I) \rightarrow RS\text{-}M(I) + \text{“}H^+\text{”} \quad (1b)$$

We can define the metal–sulfur bonding in more detail by examining the line shapes of the S(2p) core levels. In carrying out

(30) Nuzzo, R. G.; Zegarski, B. R.; Dubois, L. H. *J. Am. Chem. Soc.* **1987**, *109*, 733–740.
(31) Bain, C. D.; Biebuyck, H. A.; Whitesides, G. M. *Langmuir* **1989**, *5*, 723–727.

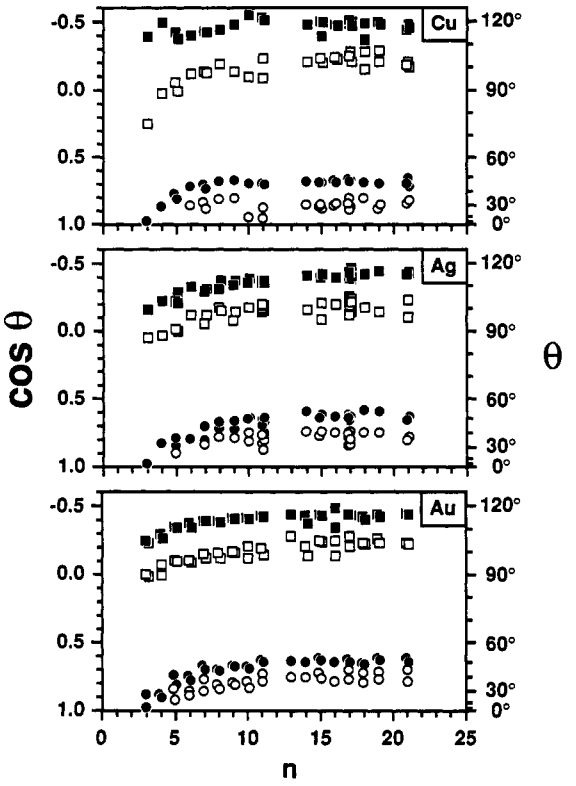

Figure 2. Wetting of monolayers of *n*-alkanethiols ($CH_3(CH_3)_nSH$) adsorbed on copper (upper), silver (center), and gold (lower) by water (squares) and hexadecane (circles). Advancing and receding angles are filled and open symbols, respectively. Each point represents the average value obtained on a slide (see Experimental Section). Exposure of copper and silver to the atmosphere was minimized prior to immersion; gold was transferred in air to adsorbate solution within 1 h of exposure to the atmosphere. Silver and gold were exposed to 1 mM solutions of alkanethiol in ethanol or isooctane for 4–12 h at room temperature under argon to form the monolayer; rinsed with ethanol, blown dry with N_2, and characterized; monolayers on copper were adsorbed from isooctane using similar procedures.

this examination, it is necessary to use data from analyses in which the X-ray exposure has been minimized. The core-level spectra indicate that the alkanethiolate monolayers degrade on prolonged exposure to X-rays. The spectra on silver and gold can be fit reasonably well, even given the noise in the spectra, as two spin–orbit-spin components of equal width (1.0 eV) whose integrated areas are in the ratio $2J + 1$ (i.e., 1:2; $J = {}^1/_2, {}^3/_2$). The spin–orbit splitting used (1.15 eV) was taken from the literature.[32] The spectra for samples on copper occasionally could also be fit within these constraints. Spectra were routinely obtained where the line widths were significantly greater (1.2–1.4 eV) and the resolution between the two components significantly poorer than those obtained on gold or silver samples. There is no unambiguous way to interpret these larger line widths; we suspect, however, that they reflect compositional heterogeneity.

Wetting Properties. Static advancing and receding contact angles of water and hexadecane (HD) were measured on monolayers prepared by the immersion of substrates in solutions of *n*-alkanethiols of various length (Figure 2). The wetting behaviors on the three metals are similar, with the contact angles of both liquids being significantly lower when $n \leq 8$ than when $n \geq 11$. Porter et al. have shown previously for monolayers formed on gold that the inferred degree of crystallinity of monolayers changes in this region.[9] We defer further discussion of the relations between wetting and structural features to later in the manuscript. The observed hysteresis ($\Delta \cos\theta = \cos\theta_r - \cos\theta_a$) is smallest for monolayers formed on gold and slightly larger on silver and copper. This increased hysteresis may reflect an underlying difference in the roughness of the two surfaces that is not detectable by SEM. In general terms, however, the wetting measurements suggest that the monolayers are all oriented, and that they expose a low-energy methyl surface[8,23–26] and, from the perspective of the outermost few ångstroms, appear to be similar.

Investigation of the Thickness of the Monolayer Films by Ellipsometry and XPS. 1. Ellipsometry. Ellipsometry is an invaluable technique for measuring film thicknesses of alkanethiols adsorbed on gold.[7–9] We attempted to measure the change in thickness on samples of copper and silver that had been exposed to air for only short intervals (<15 min) prior to exposure to an alkanethiol solution. We could, with considerable effort (see Experimental Section), obtain thicknesses on silver that could be related to the length of the adsorbate; values well outside the expected range of thickness were, however, also routinely obtained. Given the lack of reproducibility in our measurements, we are hesistant to make any structural conclusions based on relating ellipsometric thickness to the chain length of the adsorbate. Acceptable thicknesses could not be obtained on copper.

2. XPS Attenuation. XPS offers an independent method to compare thicknesses of monolayers prepared by direct exposure of the metal to an alkanethiol. In contrast with ellipsometry, characterization of the unfunctionalized interface is not required. The determination of the absolute thickness of a "thin" layer by XPS requires, at a minimum, precise values of escape depths and atomic cross sections, parameters difficult to obtain with the required accuracy. XPS does provide, however, a convenient and rapid method for comparing *differences* in relative thicknesses over a homologous series such as that represented by the *n*-alkanethiols. The logarithm of the intensity, I_M, of photoelectrons from a semiinfinite layer (>200 Å) attenuated by an *n*-alkyl overlayer is proportional to $-(nd/\lambda)$, where d is the thickness of the monolayer per methylene group, n is the number of methylene groups in each chain, and λ is the attenuation length of the photoelectrons from the underlying substrate through hydrocarbons.[33] A plot of ln (intensity) versus n provides both a qualitative assessment of the regularity of the thickness of monolayers prepared from different length alkanethiols and a comparison between monolayers formed on different metals. Because the escape depth (λ) is also a function of the kinetic energy of the photoelectron,[34] we selected specific core level peaks based on both their cross section and proximity to peaks of other metals.

The intensity of photoelectrons arising from the underlying substrate of kinetic energies of ~1125 eV ($Au(4d_{3/2})$ = 1134 eV, $Ag(3d_{5/2})$ = 1119 eV) and ~1400 eV ($Au(4f_{7/2})$ = 1402 eV, Cu(3p) = 1412 eV) are plotted in Figure 3 for monolayers prepared from *n*-alkanethiols of different lengths.[35] These plots follow the expected logarithmic relationship. The intensity of photoelectrons for monolayers on silver and copper attenuate more rapidly (by ~20%) than for monolayers on gold. This difference suggests that the films formed on copper and silver are each ~20% thicker than those formed on gold. This observation is consistent with the differences in molecular orientation inferred from infrared spectroscopy (see below).

Investigation of Film Structure and Molecular Orientation by IR Vibrational Spectroscopy. 1. Observed Spectra of Monolayers. IR spectra of the various monolayers were obtained using a single reflection geometry (~85° angle of incidence) as described in the Experimental Section using p-polarized light. In earlier papers, quantitative analyses of such data have been presented for monolayers of various substituted alkanethiols and dialkyl disulfides on gold.[12,36] The present study seeks to present a quantitative correlation of thin-film structure as exhibited in a homologous series of adsorbates across these related substrates. To facilitate these analyses, the previous computational proto-

(32) Salaneck, W. R.; Lipari, N. O.; Paton, A.; Zallen, R.; Liang, K. S. *Phys. Rev. B* **1975**, *12*, 1493–1500.

(33) Bain, C. D.; Whitesides, G. M. *J. Phys. Chem.* **1989**, *93*, 1670–1673.

(34) Seah, M. P.; Dench, W. A. *Surf. Interface Anal.* **1979**, *1*, 2–11.

(35) A similar slope was obtained for alkanethiols (C_6–C_{18}) adsorbed on copper from ethanol even though the monolayers exhibited significant contact angle hysteresis.

(36) Nuzzo, R. G.; Fusco, F. A.; Allara, D. L. *J. Am. Chem. Soc.* **1987**, *109*, 2358–2367.

Table II. Description of Vibrational Modes of C–H Stretching for Polycrystalline Alkyl–S Chains $C_{16}H_{33}S$ – $C_{22}H_{45}S$[a]

mode description[b]	peak frequency (cm^{-1})[c]	assigned direction of transition dipole moment matrix element in molecular coordinates
CH_3 asym (ip), (r_a^-)	2964	ip of CCC backbone, ⊥ C–CH_3 bond
CH_3 asym (op), (r_b^-)	2954	⊥ CCC backbone plane
CH_3 sym, r^+ (FRC)	2935	∥ to C–CH_3 bond
CH_2 asym, d^- (α)	2925	⊥ CCC backbone plane
CH_2 asym, d^-	2918	⊥ CCC backbone plane
CH_2 sym, d^+ (FRC)	2895–2907	ip CCC backbone plane, ip HCH plane
CH_3 sym, r^+	2879	∥ to C–CH_3 bond
CH_2 sym, d^+ (α)	2853	ip CCC backbone plane, ip HCH plane
CH_2 sym, d^+	2850	ip CCC backbone plane, ip HCH plane

[a] Based on data taken for $[C_nH_{2n+1}S]_2$ samples used for optical function determinations. [b] Abbreviations used: asym = asymmetric or antisymmetric, sym = symmetric, ip = in plane, op = out of plane, FRC = Fermi resonance splitting component, α = CH_2 groups located at either end of the alkyl chain, ∥ = parallel, ⊥ = perpendicular. [c] Peak frequency is taken as that from the imaginary optical function (k) spectrum. Peak frequency values for modes of intensities too weak to measure directly have been assigned using average values taken from previously compiled assignments (ref 9, 12, 36, 37). These values were subsequently used in the fitting routines used to generate the components of the simulated spectra (see supplementary material).

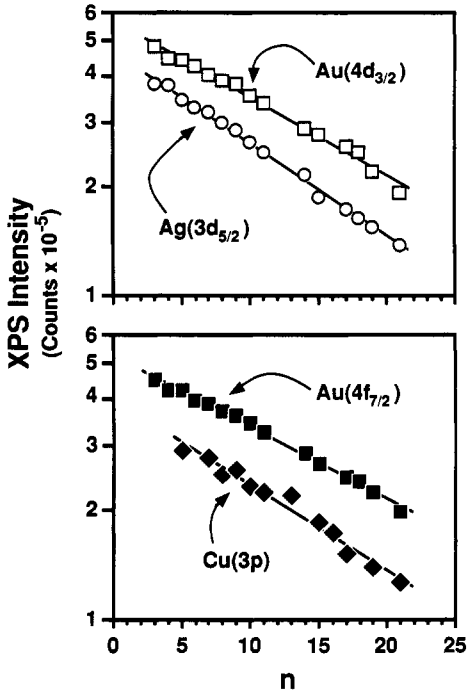

Figure 3. Intensity of photoelectrons due to the underlying substrates for monolayers on gold, silver, and copper formed after 1 h exposure to 1 mM solutions of n-alkanethiols ($CH_3(CH_2)_nSH$). The upper figure provides comparison of monolayers formed on gold and silver, the lower on gold and copper. The points represent single measurements. The data sets have been offset vertically to enable comparison; the slope is the parameter that is important here. The kinetic energies of the photoelectrons in each graph are similar: (upper) $Au(4d_{3/2})$ = 1134 eV, $Ag(3d_{5/2})$ = 1119 eV; (lower) $Au(4f_{7/2})$ = 1402 eV; Cu(3p) = 1412 eV. Lines were obtained by least-squares analysis and gave the following slopes (see text): $Au(4d_{3/2})$, –0.021; $Ag(3d_{5/2})$, –0.025; $Au(4f_{7/2})$, –0.020; Cu(3p), –0.024.

cols[12,36,37] were modified (see below). Further, since we anticipated that the differences between specific adsorbates of interest to us might be small, our earlier work was reexamined with the intention of minimizing experimental errors that complicate a precise quantitative comparison of the data obtained from different substrate materials. The analyses that follow are based on multiple sample preparations conducted in three different laboratories and spectral data acquired on two different instruments. The *largest* variations we observed for comparable instrument optics are compatible with the statistical variation inherent in multiple samples. The error bars appearing in the figures reflect the scatter dominated by effects due to independent measurement of multiple samples. It is important to note that the data shown below reflect our specific optical design. Large differences in absolute spectral intensity will result if even slightly different beam divergences and angles of incidence are employed.[38]

The infrared data for the series of monolayers on copper, silver, and gold are shown in Figure 4. The data shown for copper are for the more well-defined structures we have obtained (a representative example of spectra obtained for ill-defined monolayers on copper is given in the supplementary material). The sets of data reveal substantial variations in the C–H vibrational mode intensities as a function of chain length for gold as compared to the other two systems of monolayers (copper, silver). Given the close similarity of the copper data to that of silver, we will restrict our discussion to the better-behaved silver system (although similar discussions would pertain for this specific copper data set). We will discuss for gold the CH_3 mode intensities first and follow with an examination of those of the methylenes. The basis of the assignment of the spectral features to specific vibrational modes has been reported previously[12,36,37] and will not be repeated here. Details of these fairly complex fittings and assignments are given in the supplementary material. Table II presents exact descriptions of the assignments, the approximate position of the band, as well as transition dipole directions for the mode as expressed in molecular coordinates. The latter information will be used for calculations of structure discussed in the next section. Our quantitative interpretations of molecular orientations will be restricted to analyses based on modes appearing in this high-frequency region. The lower frequency modes, while rich in information (see below), are sufficiently weak in intensity as to preclude quantitative analysis.

The strongest of the CH_3 modes in this region of the spectrum is the symmetric methyl stretch (r^+), which is split by Fermi resonance into two separate bands appearing at ~2878 and ~2935 cm^{-1}, and the in-plane asymmetric stretch (r_a^-) appearing at 2964 cm^{-1}. The out-of-plane asymmetric stretch (r_b^-), which occurs prominently at 2954 cm^{-1} in the polycrystalline bulk phase spectra, is weak in the monolayer spectra; this mode is a weak shoulder on the r_a^- band. The line shapes do not appear to vary significantly across this series of monolayers, allowing band intensities to be estimated for most bands (r_b^- excepted) by the intensity at the peak maximum. Figure 5 shows the intensity data of the r^+ (2877 cm^{-1}) and r_a^- (2963 cm^{-1}, contains a small contribution from r_b^- absorption) bands for the C_{16}–C_{20} films on gold and silver. On gold, the data are given normalized relative to the value of the intensity of the selected mode for the C_{16} film. The theoretical plots shown for gold of the modulation of these deviations in intensity are based solely on the changes in *geometry* of the CH_3 group predicted for two possible models of chain

(37) Allara, D. L.; Nuzzo, R. G. *Langmuir* **1985**, *1*, 52–66.

(38) In particular, the angle of incidence must be correctly set within less than 1°, the f/number of the beam must be fixed at a high value, ~f/15 – f/20 for our two instruments, and stray light must be excluded from collection of the reflected beam off the sample. We (D.L.A., R.G.N.) observed fluctuations as much as a factor of 2 between misaligned, fast optics and the configuration above. Additional deviations could also involve detector nonlinearities for high throughput configurations.

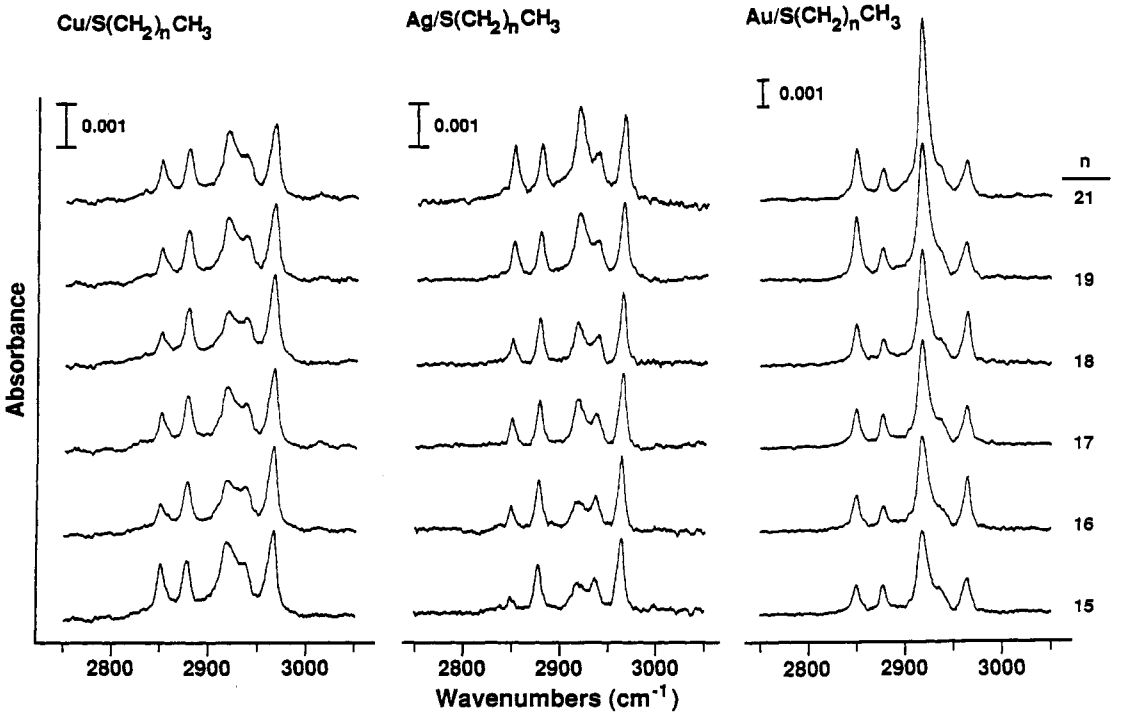

Figure 4. IR spectra of monolayers derived from exposure of surfaces of copper, silver, and gold to *n*-alkanethiols ($CH_3(CH_2)_nSH$).

structure and not on changes in the vibrational states. These models will be discussed in detail later in the manuscript. The experimentally observed fluctuations in odd–even intensities are striking. It is also obvious that this experimental behavior presents an important criterion for determining the validity of various structural models. In an earlier publication,[12] these variations were noted qualitatively and used to assign a constant fixed direction of chain tilt with a consequent odd–even dependence of the orientation of the C–CH_3 bond with respect to the normal to the surface. This point will be discussed in detail later in the manuscript.

Figure 5 also shows that the r^+ and r_a^- band intensities (absolute) on silver exhibit, to within experimental error, no significant modulation with chain length. This difference between the spectra obtained on silver (and similarly on copper) and on gold strongly suggests a difference in structure of monolayers on these supports; those on silver (and copper) indicate that the projection of the C–CH_3 bond on the normal to the surface is invariant with chain length.

The C–H stretching mode intensities (absolute) of the CH_2 group d^+ and d^- modes exhibit a linear dependence on chain length for monolayers supported on gold and silver (plots are given in the supplementary materials).[39] No odd–even variations are evident, suggesting, within the experimental uncertainty of the measurement, that there exists a constant chain orientation on the surface for these films, one that differs in magnitude for silver and gold.

2. Determination of Optical Functions. Descriptions of the methods used for determining precise optical functions, an overview of relevant error analysis, and representative data used in the theoretical modelling are given in the supplementary materials.

3. Calculation of Average Molecular Orientation in Monolayer Films on Copper, Silver, and Gold. The theoretical basis for deriving an average orientation of molecules in monolayers from IR spectra of metal supported films has been presented in detail elsewhere.[37] As presented then, the essential operations involved were (1) the determination of a set of isotropic optical functions applicable to the monolayer films;[40] (2) the experimental determination of the thickness of the film from ellipsometry (or other independent method); (3) simulation of an experimentally appropriate monolayer spectrum (i.e., accounting for reflection geometry, etc.) using the above parameters; (4) assignment of each absorption feature to a single or combination of contributing vibrational modes, each possessing a matrix element corresponding to a transition dipole moment with a specific direction in molecular coordinates; (5) assignment of the discrepancies in band intensities between the isotropic simulation and the experiment to average orientations of each of the elements of the transition dipole moments using a framework of classical electromagnetic theory; and (6) converting the dipole orientations in molecular coordinates to a molecular geometry on the surface via transition dipole directions in molecular coordinates (Table II). It is, of course, critical that there exists a transferability between the optical functions used (derived from a bulk state) and those relevant to the phase state of the monolayer. Errors in the ellipsometrically determined thickness are also of concern, although, for typical errors of less than several ångstroms, the influence on the determined orientations is generally small (values of thickness used are given in the Experimental Section).

The procedure used for numerical comparison in the present study differs in significant detail from that reported previously. The present study utilizes complete spectral simulations; a descriptive overview of the method is given in the supplementary material.

Simulations were performed for a wide range of surface geometries of the adsorbed molecules. The range of structures to be considered was narrowed somewhat by noting that the experimental spectra (presented earlier) suggest the placement of the chains in a crystalline-like environment. Indeed, it has been demonstrated by several techniques that the monolayers on gold are ordered.[10,11] Therefore, only structures with alkyl chains in an all-trans conformations were considered initially. In the latter portions of the manuscript, we will present simulations in which this all-trans constraint has been relaxed to allow gauche conformations at the terminal CH_2 group. With regard to the present focus on all-trans chains, the copper system presents a significant challenge to analysis. The best samples give spectra virtually identical with those found on silver. Their analysis would thus

(39) Linear least-squares fits to the intensities of the d^+ and d^- modes versus chain length for monolayers supported on gold and silver intersect zero intensity at chain lengths significantly greater than zero. Plots and further discussion are included in the supplementary materials.

(40) Tables of the optical functions for all the alkanethiols reported in this study (C_{16}–C_{20} and C_{22}) are available on request (D.L.A.).

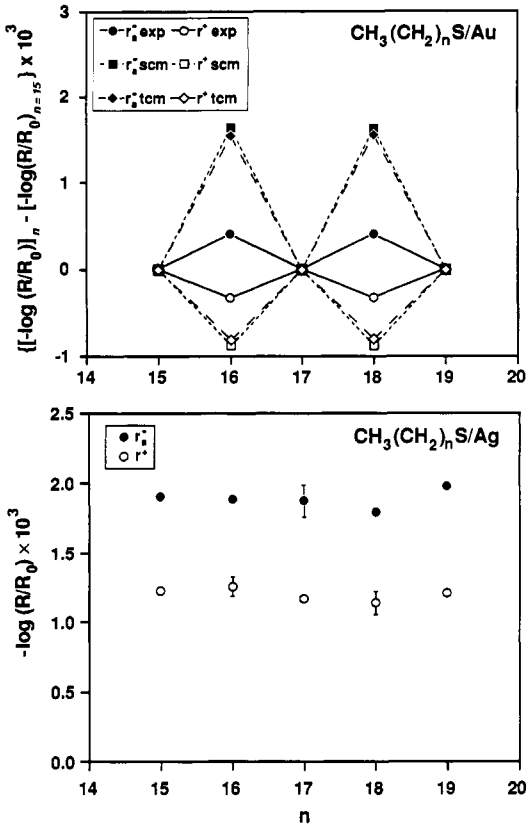

Figure 5. Intensities of methyl stretching modes, r^+ and r_a^-, for *n*-alkanethiols ($CH_3(CH_2)_nSH$) adsorbed on gold and silver. The experimental values of r_a^- contain a small contribution from the unresolved intensities of the r_b^- modes. The upper panel displays experimental and calculated intensity deviations (normalized to the band intensities found for a monolayer of hexadecanethiol adsorbed on gold) of the methyl stretching modes, r^+ (open) and r_a^- (filled), for *n*-alkanethiols adsorbed on gold. The calculated intensities are based on various structural models that are discussed in the text: exp (experimental value), scm (single-chain model), tcm (two-chain model). The lower panel displays the experimental intensities of r^+ and r_a^- for *n*-alkanethiols adsorbed on silver. The lack of any change in the intensities of the symmetric and asymmetric methyl stretching modes for odd and even values of *n* on silver sharply contrasts that observed on gold (upper panel).

be that same as that which follows for silver and is therefore not repeated. The "disordered" materials characterized by the type of spectra shown in the supplementary material cannot be treated under the constraints initially imposed on this analysis, namely, that there does not exist a reference phase from which we can derive with certainty suitable optical functions; the spectra are neither crystalline nor liquid-like in character. The data suggest that there exists in these materials some fraction of extended trans segments as well as considerable densities of gauche conformations. This might imply that lower coverages of adsorbate may be present on these surfaces than is to be found on those bearing closest packed chains. By assuming a coverage, the weighting of this fit as domains of liquid and solid-like material could produce a convergent simulation, but, given the ill-defined nature of these phases, there seems little justification for doing so.

Figure 6 shows a schematic diagram of an all-trans chain as well as the coordinate system used to define the orientations of the chains. The chain tilt angle, α, is defined as the cant of the long axis of the trans-zig-zag polymethylene chain relative to the surface normal direction (z). The chain twist, β, is the twist of the plane of the chain ($+\beta$, counterclockwise rotation) around the chain axis. This coordinate system, based on the typical Euler convention, is sufficient to describe the chain geometry of a uniaxial system (recall that only the z component of the transition dipole moments gives rise to absorption; all x and y orientations are equivalent and thus the system is uniaxial). In order to describe both odd and even chains with this one diagram, the

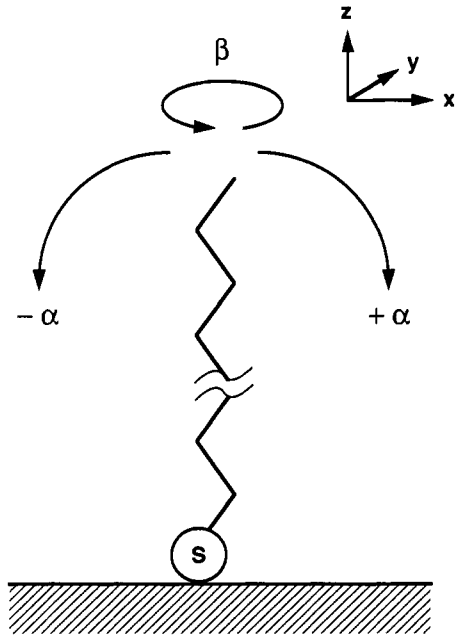

Figure 6. Schematic diagram of an all-trans chain in an *n*-alkanethiols monolayer on a surface. The coordinate system used to define the orientations of the chain, the cant angle α, and the chain twist β are shown along with their relationship to the surface coordinates.

convention was adopted in which the metal–S–C geometry is conserved for both types of chains. The figure as drawn describes the direction of the C–CH_3 bond as a positive tilt for a chain with an odd total number of carbon atoms (even number of CH_2 groups). The convention thus requires that α and β be specified for an even chain in which the initial C–CH_3 bond is tilted in the opposite (negative) direction.

The data above suggest that all the chain lengths examined formed self-consistent structures. In the interests of brevity, therefore, fits to only a selected series of spectra are presented. We will consider first the molecular orientations of monolayers on silver, and then compare these to those on gold. For all the cases considered in the simulation models, excellent fits to the experimental spectra could be found for the CH_2 C–H stretching mode adsorptions (d^+ and d^-). In no case, however, could a simultaneous convergence of the CH_3 C–H stretching modes (r^+, r_a^-, r_b^-) be achieved; the total errors could be minimized to values approaching ~20–30% of the total methyl band intensities (see discussion above). On the basis of the observed fitting errors, best fit convergence is defined in terms of the d^+ and d^- modes, which are used to determine the tilt (α) and twist (β) angles of the chains (see Figure 6). It is important to note that the symmetry of the CH_2 groups about the chain axis precludes the use of the d^+ and d^- modes to determine the absolute sign of the tilt angle, α. This latter parameter, which establishes the structural features of the film surface (i.e., the direction at which the terminal C–C bond protrudes into the ambient), has been arrived at using observations of the odd–even behavior of the CH_3 mode intensities and will be detailed below.

The errors associated with the best fits for a C_{18} thiolate monolayer on silver are illustrated in Figure 7. The analysis suggests that these materials are, in fact, well modeled by the optical constants of the bulk phase and exhibit a small but appreciable cant angle (α) of 13°. The stiffness of the fit is clearly demonstrated by the observation that variation of α and β by even ±2° (not shown) greatly degrades the fit. The fits to the other silver monolayer data sets were equally good with a range of the absolute values of the cant angles ($|\alpha|$) varying from 11° (C_{16}) to 14° (C_{20}); the twist angles, β, were also similar ranging from 42° to 44° (C_{19}). These variations are well within the accuracy of this method. Inspection of the data in Figure 7 also reveals that the sign of the cant angle is strongly constrained by the simulations. Even though the absolute intensity of the methyl

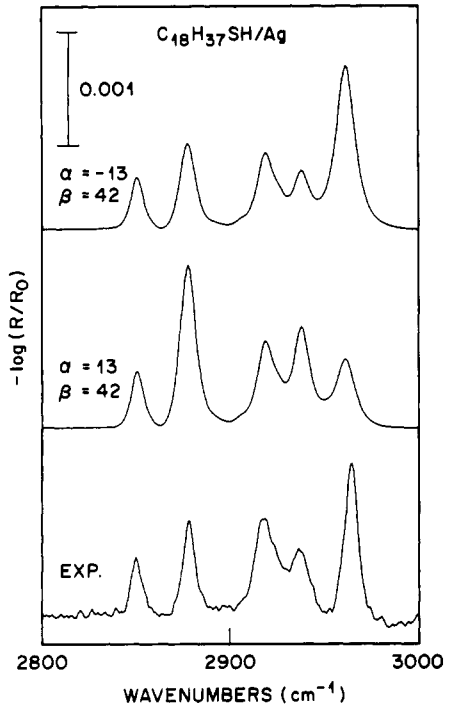

Figure 7. Experimental (lower) and calculated IR spectra of octadecanethiol adsorbed on silver. Calculated spectra having cant angles, α, of −13° (upper) and +13° (lower), and twist angles, β, of 42° are presented. The differences in the calculated spectra suggest that α is −13° (as defined by Figure 6). Specific interpretations are discussed in the text. The calculated spectra are based on a single chain model (see text).

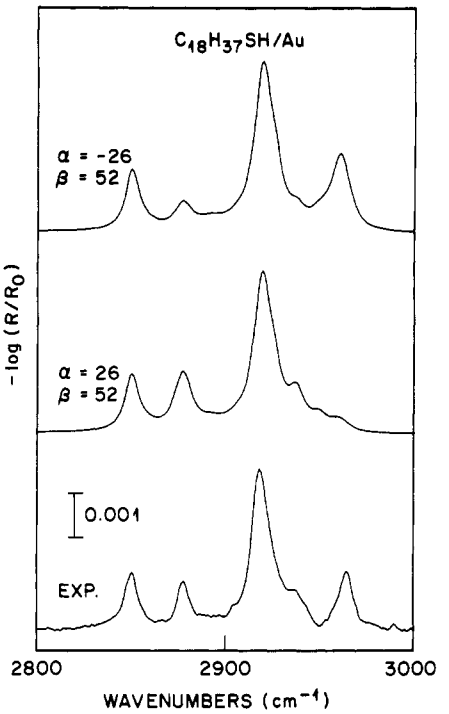

Figure 8. Experimental (lower) and calculated IR spectra of octadecanethiol adsorbed on gold. Calculated spectra having cant angles, α, of −26° (upper) and +26° (lower), and twist angles, β, of 52° are presented. The two simulations provide equally good fits that do not allow absolute assignment of α. The calculated spectra are based on a single-chain model (see text).

modes suggests the importance of effects other than orientation in determining the band intensities (especially r_b^-), the fits fail most profoundly for positive values of α. This result, when viewed in the context of the data presented in Figure 5, suggests that the surface projection of the methyl group does not vary in the silver-supported monolayers as one changes the length of the chain. *Stated differently, the fits, given the conventions adopted in Figure 6, require negative signs of α for odd numbers of methylene groups and positive ones for even numbers.* Discussion of the import of this observation is deferred to later in the manuscript.

Whereas the spectral intensities of the monolayers formed on silver could be fit by the use of a single-chain model, viz., one average chain geometry representing the structure of all the chains in the monolayer ensemble, the gold system requires the consideration of more complex models. In recent studies, it has been found that the spectra of these monolayers are strongly temperature dependent and reveal two important structural features.[41] First, the chains, even though well described as being "crystalline-like", do indeed contain appreciable quantities of gauche conformations; these are concentrated at the chain termini. Second, spectra at low temperature exhibit factor group splittings which suggest that, at least at $T \lesssim 220$ K, the ordered structure adopted contains two chains per unit cell. These observations are supported by recent molecular dynamics simulations on this monolayer system.[42] Thus, it is required from the outset that the models used incorporate two-chain geometries and allow the population of terminal CH_2 gauche conformations. Because of the demands placed on the accuracy of the spectral simulations by such models to distinguish the subtle numerical differences expected, added emphasis was placed on the measurement and use of improved n, k data sets, data unavailable prior to this work (see above and supplementary material).

We start with a consideration of the simplest case, a single-chain model. Using a best fit criteria based on the d^+ and d^- modes, the single all-trans chain structure derived for *n*-alkanethiolate monolayers on gold has an average cant angle, α, in a narrow range of 26–28° and a twist, β, of ~52–55°. Specific simulations are shown in Figure 8 for an octadecanethiolate monolayer for both positive and negative values of α as well as the experimental data for reasons of comparison. As before, the calculated data for this particular monolayer yields fits in a narrow range of values for α (shown here for $\alpha = \pm 26°$) and β (52°); changing these values by ±2° seriously degrades the quality of the fits for the d^+ and d^- modes.

On first glance, the data in Figure 8 might be construed as indicating that the proper value of the cant angle is $\alpha = -26°$, the fit to methyl r_b^- mode being somewhat closer for this sign of α. The weighted errors are actually comparable in the two fits, when one takes proper account of the total intensity of the r^+, r_a^-, and r_b^- modes. These specific simulations thus are insufficient in and of themselves to choose between the signs of α. The larger data set (C_{16}–C_{22} thiols) does provide, however, a basis on which to make such an assignment. The intensities of the methyl C–H stretching modes fluctuate with varying chain length (Figure 5), revealing that the surface projection of the methyl groups is not conserved as one adds an additional methylene group to the chain; odd and even chains yield different methyl orientations although within these latter groups the structures appear to be similar. The simulations reveal that the qualitative character of these intensity fluctuations are best described within the confines of the single-chain model by assigning a positive sign to the chain cant angle, α (Figure 6), which is conserved for all chain lengths. We have noted in an earlier publication that there exist significant perturbations of optical functions of the monolayer for groups located at the ambient interface relative to the bulk reference phase.[12,41] These effects are sufficiently large even for the fairly simple, nonpolar methyl group (intermolecular interactions by dispersion forces) so as to prevent definitive calculations of an average methyl group orientation. This perturbation could involve in principle both the magnitude and direction of the oscillating dipoles. On the assumption that the directions do not change, a simple calculation can be made from the experimental data as to the changes in intensity required to allow the exact quantitative representation

(41) Nuzzo, R. G.; Korenic, E. M.; Dubois, L. H. *J. Chem. Phys.* **1990**, *93*, 767–773.
(42) Hautman, J.; Klein, M. L. *J. Am. Chem. Phys.* **1989**, *91*, 4994–5001.

of a specific data set. The calculated modulations of CH_3 C–H stretching mode intensities shown in Figure 5 were derived on the basis that the Au–S–CH_2 bond angle is constant for all chain lengths. On this basis, the only difference between odd and even chains can be the orientations of the C–CH_3 bond with respect to the surface and, hence, the transition moment directions of the r^+, r_a^-, and r_b^- modes. With these assumptions, the latter are exactly defined for both odd and even chains for a chosen tilt/twist configuration (Figure 6), and the ratio of the mode intensities can be exactly calculated for an even chain versus an odd on the basis of the change in $\cos^2 \theta_{mz}$ (where θ_{mz} is the angle of the transition moment with respect to z axis for a given mode of a particular chain length[37]). The calculated moduli shown in Figure 5 were derived in this manner (the calculated changes in r_a^- and r^+ are referenced to the intensities for the even chain). It is evident that the discrepancy is quite substantial. Most of this discrepancy appears to be due to the assumption underlying the simple all-trans single-chain model.

As has been already noted, the use of a two-chain model is more consistent with current evidence that supports a low-temperature structure similar to a bimolecular monoclinic hydrocarbon phase with the planes of the C–C backbone at ~90° to one another.[41] From this starting point, two structural classes were developed for spectral simulations: (1) the low-temperature structure with two contributing average chain structures, each of equal population with all-trans conformations; and (2) the high-temperature structure, identical with the above all-trans model except for allowing the population of both trans and gauche conformations of the *terminal CH_2 groups* of both chains in an independent, uncorrelated fashion.[43]

One distinct result obtained from the fitting procedure is that a family of structures all give nearly identical minimum error fits to the CH_2 modes for values of ϕ bounded by $0 \leq \phi \leq 82°$ with each value of ϕ associated with a specific pair of β_1, β_2 values. For $\phi > 82°$, the fits worsen. Since the structure of a orthorhombic crystalline subcell would require $\phi = 90°$, the upper limit value of $\phi = 82°$ was selected as the most physically real value.[44] For this constraint, the all-trans, two-chain model yields chain twists of 50 and −48°. The corresponding simulated spectrum, shown in Figure 8, while producing an excellent fit for the CH_2 modes, clearly yields a poor fit to the intensity profiles of CH_3

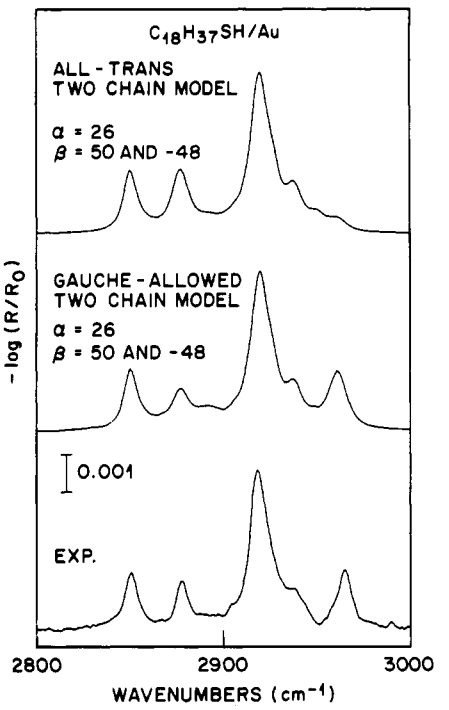

Figure 9. Comparison of experimental (lower) and calculated spectra of octadecanethiol adsorbed on gold. The calculated spectra are based on a two-chain model. The chains were assumed to be all-trans in the upper simulation and allowed to adopt gauche conformations at the terminal methylene group in the lower. Specific discussions are presented in the text.

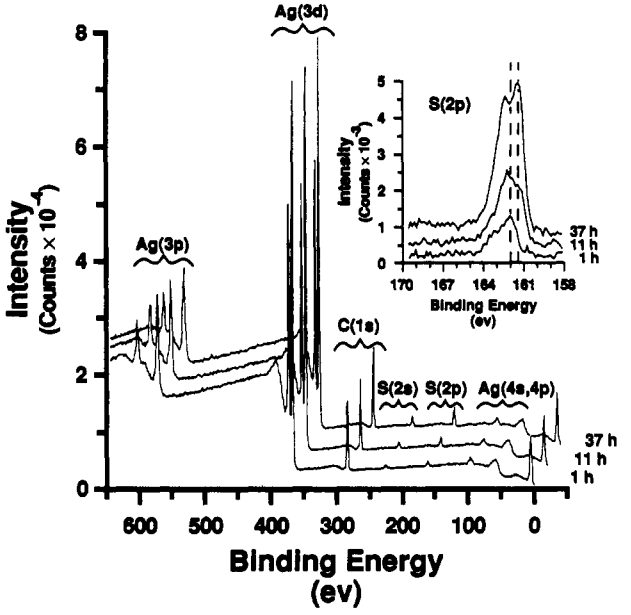

Figure 10. XPS spectra of silver samples exposed to 1 mM solutions of octadecanethiol in isooctane for 1, 11, and 37 h each. With continued exposure, the sulfur signals become more intense with "growth" of peaks at lower binding energies (see inset); no other changes in the spectrum were observed. The S(2p) spectrum for the sample exposed to solution for 37 h could not be fit with the two spin–orbital-split components of a single sulfur-containing species. This spectrum was, however, easily fit by two pairs of spin–orbital-split components; one pair resembled the spectrum given for 1-h exposure suggesting that the thiolate remains present while an additional species (one at lower binding energy) had been incorporated. We believe the new sulfur-containing species to correspond to the formation of a thin film of Ag_2S at the silver/monolayer interface. The wettabilities of the samples were essentially indistinguishable and confirmed that the hydrocarbon films on them are oriented.

(43) To describe the geometry of these models, the following conventions were adopted. For a given pair of chains, an angle between planes of the chain, ϕ, was selected and the common axis between the planes allowed to rotate (equivalent to twisting the chains in concert by the same amount) and tilt away from the surface normal. It follows that, for a pair of chains indexed as 1 and 2, $\phi = |\beta_1 - \beta_2|$ and $\alpha_1 = \alpha_2 \equiv \alpha$. Since the plane of the chains can be rotated by 180° with no effect on the optical response of the CH_2 modes, one can equivalently specify ϕ as $180° - |\beta_1 - \beta_2|$. As a convention we choose the smallest value of ϕ. The strategy for the best fit-simulation procedures for both models involved: (1) fixed α to be that determined from the best fit of the single chain model (given above) and (2) variation of β_1 and β_2 independently between +90° and −90° (one negative value of β is required to produce the proper methyl surface corrugation; see below). In addition, for the gauche-allowed model, β_1 and β_2 for the best fit all-trans model were selected and fixed while a large variety (~10^4) of conformational populations were searched independently for each chain in a collection of 20 independent unit subcells (2 chains per unit subcell). The monolayer thus was represented by 40 chains (20 with β_1 and 20 with β_2), with each chain independently populating one of three conformational geometries, trans, gauche (1), and gauche (2), with each conformation exhibiting a different contribution to spectral intensity.

(44) The numerical precision in these calculations is such that a range of ϕ values between ~76 to 85° (or equivalently 180° − (76 to 85°) = 104 to 95°) will give a reasonable fit to the intensities of the CH_2 modes. There is an interesting and simple geometric relationship that can be derived relating the twist angle of a single chain model, β_s, to the twist angles of the two chain model, β_1 and β_2, for the condition that the overall geometric factors (see supplementary material, footnote 7) for the d^+ and d^- modes, $G^{d^+}(\alpha, \beta)$ and $G^{d^-}(\alpha, \beta)$, each be identical, respectively, in both models:

$$|\beta_1 - \beta_2| = \phi \leq |\Phi(\beta_s) - 2\beta_s| \quad (2)$$

In line with our earlier convention of choosing ϕ, $\Phi(\beta_s) = 0°$ when $0° \leq \beta_s < 45°$ and $\Phi(\beta_s) = 180°$ when $45° \leq \beta_s < 90°$. The condition required by this inequality is that the models give identical simulated CH_2 spectra. Thus, for an orthorhombic unit subcell with $\phi = 90°$, it follows that $\beta_s = 45°$ and all two-chain models can be replaced by one single-chain model. Another result is that for $\beta_s = 52°$, the average result derived for a single-chain twist on gold in the text, the inequality requires $\phi \leq 76°$, close to the range found numerically of ~76–85°.

modes (indeed, ones no better than the single-chain model). Using these fixed values of α, β_1, and β_2 which provide quantitative simulation of the CH_2 modes, the fitting process revealed a second distinct result, namely, that a large number of best fits to the CH_3 modes exist with nearly a random mixture of allowed gauche populations. In the above, the worst fit to the total intensity of the CH_3 modes is obtained for zero gauche states, viz., the all-trans model above. The calculated spectrum shown in Figure 9 is derived from a model with a total conformer population of 45% gauche and 55% trans in the collection of 40 chains sampled. In general, even a small percent of gauche states can decrease the fitting error associated with the CH_3 modes by a factor of $\sim$5. It should be noted that, of course, certain combinations of conformational states give poor fits but none worse than the all-trans model. Thus, randomization of terminal conformations can only lead to improved fits. The final point to note is that no combination of conformational states sampled could provide a less than $\sim$10% error between the spectral intensities of the calculated and observed total CH_3 modes.

It must be emphasized, therefore, that precise quantitation to better than $\pm$10% requires consideration of perturbations of the optical constants of the CH_3 group at the air/monolayer interface relative to the CH_3 groups in a crystalline reference material. Such effects probably exist and should be considered to be in the range of $\sim$10% of the total values of k (as suggested by the fitting errors above). The significant point remains, however, that the best fits are consistent with a population of gauche conformations at the chain ends, as independent experiments suggest exist.[45]

Influence of Extended Immersion Times or Exposure to Air on the Nature of Self-Assembled Monolayers on Silver and Copper. We have observed that, while the nature of the monolayers formed on gold are insensitive to changes in the immersion times in the adsorbate solution over periods of several weeks, those formed on silver and copper can differ in considerable detail. We have begun to examine these features in greater detail and can report some initial findings. Extended exposure of copper and silver surfaces to solutions containing alkanethiols results in films that appear too thick by ellipsometry; the thicknesses inferred are too large to be explained by adsorption of a monolayer (see above). We found, by XPS, that the films formed on silver, after extended exposure to the adsorbate solution, contained no oxygen and the amount of carbon was similar to that found on samples exposed for shorter immersion times (Figure 10). The major difference between the XPS spectra is the increased amount of sulfur present with continued exposure to the alkanethiol solution.[46] The amount of sulfur (relative to the amount of carbon) is too large to be explained if sulfur is only present as alkanethiolate. We believe formal C–S bond cleavage has occurred to generate a thin film of Ag_2S at the silver/monolayer interface;[47] it may be this reaction that is responsible in part for the anomalous ellipsometric thicknesses mentioned earlier. Surprisingly, the wettabilities by water and hexadecane of the hydrocarbon films remained similar to those obtained after more limited exposures and were consistent with the presence of a densely packed, methyl surface. We believe that during the formation of an interphase of Ag_2S, an organized, oriented alkyl thiolate assemblage continues to exist (see below). On copper, similar increases in sulfur content were observed, suggestive of formation of copper sulfide; however, the surfaces routinely became pitted and did not allow characterization by wetting.

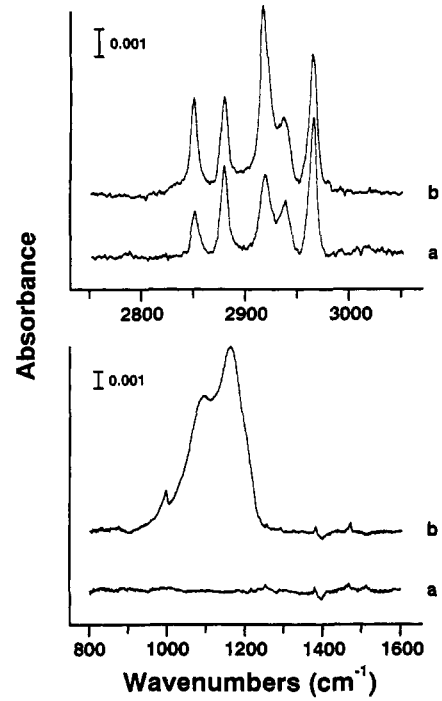

Figure 11. IR spectra of monolayers prepared on silver by exposure to octadecanethiol in ethanol, after different intervals of subsequent exposure to the atmosphere (a, $\sim$1 h; b, $\sim$2 b). The high-frequency (upper panel) and low-frequency (lower panel) regions of the IR spectra display the changes that develop with time. The high-frequency region shows that the hydrocarbons chains have become oriented less perpendicularly but remain in a crystalline-like environment. The low-frequency region and the XPS spectra (Figure 12) show that some of the thiolate head groups have been oxidized to sulfonates.

Upon extended exposure of an alkanethiolate monolayer on silver or copper to the atmosphere, the sample changes; a representative example of the IR spectrum of such a material is shown in Figure 11. This sample was obtained after a few days of exposure of an octadecanethiolate monolayer on silver to air. Three features of the data are of particular significance. First, the peak positions of the CH_2 C–H stretching modes are consistent with the presence of a dense crystalline-like phase (d^+, 2850 cm^{-1}; d^-, 2917 cm^{-1}). Second, the corresponding intensities suggest that the chains are more highly canted than those described above. Third, the low-frequency portion of the spectrum exhibits a very intense band centered at $\sim$1200 cm^{-1}. Using the optical constants of an *n*-alkyl disulfide as a basis set, we roughly estimate that the chain cant, α, for this new phase is $\sim$18° with the twist $\beta \cong 45°$. We urge caution in interpreting this result, as the head group on the chain is now presumably not thiolate (see Discussion below) and perturbations of n and k are expected to result. It does seem safe to conclude, however, that the orientations of the methyl groups at the ambient surface differ in significant detail from those supported by a thiolate head group.

The XPS data shown in Figure 12 for a monolayer on copper exposed to the atmosphere suggest that some of the sulfur atoms in this monolayer are oxidized as judged by the additional $S(2p_{3/2})$ core level at a binding energy of $\sim$167.5 eV. An increase in the intensity of the O(1s) core level region is also observed. We believe the species present on the surface to be an alkyl sulfonic acid, presumably present as a sulfonate anion. The binding energy of $S(2p_{3/2})$ is comparable in position to that obtained by treating an oxidized silver or copper surface with an alkyl sulfonic acid (see Table I). We have observed on silver similar oxidation of

(45) There is a further subtle correction in the simulated spectral intensities of the d^+ and d^- bands which should be made where gauche conformations are introduced into the chain end. Because these modes are delocalized (see supplementary material), the loss of one trans conformer in an all trans chain by conversion to a gauche state can diminish the overall band intensities by an amount greater than the fraction of the total CH_2 groups which the altered group represents. For the case of an originally all-trans $-(CH_2)_{17}-$ chain converted to a 1 gauche kink chain, thus we expect $I_g/I_t \leq 17/18 \approx 0.94$ or a more than 6% drop in intensity. A reasonable upper bound is probably $\sim$10% (Snyder, R. G.; Maroncelli, M.; Strauss, H. L.; Hallmark, V. M. *J. Phys. Chem.* **1986**, *90*, 5623–5631). Considering that probably only half ($\sim$45% for the fit given in Figure 9) the chains have gauche kinks, the effect of the drop in intensity in the simulation is to increase the chain tilt α and a change in the tilt from 26° to $\sim$29° will accomplish this. Although such a correction cannot be made rigorously because of the lack of actual gauche state populations and the exact intensity relationship, the size of the correction is reasonable in terms of physically acceptable values of α.

(46) No differences were noted in the character of the $Ag(3d_{5/2})$ core level upon extended exposure to the alkanethiol solution; however, the binding energies of $Ag(3d_{5/2})$ for Ag_2S and bulk Ag are similar ($\Delta BE \leq 0.1$ eV).[38]

(47) Cleavage of C–S bonds by silver of thiols, disulfides, and sulfides has been reported.[4]

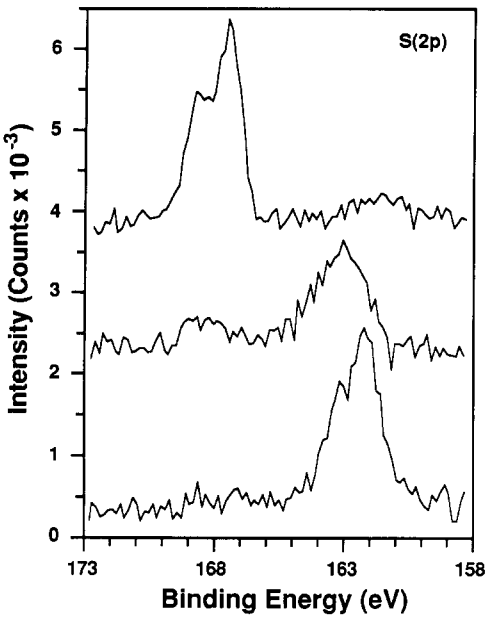

Figure 12. Effect of exposure to atmosphere on XPS spectra of octadecanethiolate monolayers on copper (bottom, <1 h; middle, ~2 wk). The upper spectrum is of a silver surface derivatized in an isooctane solution of hexadecanesulfonic acid, presumably adsorbed as the sulfonate anion, and is provided for comparison. All spectra (40 scans) were referenced to C(1s) = 284.80 eV. The lower spectrum exhibits a S(2p) envelope consistent with a thiolate attachment; the sample exposed to atmosphere for 2 weeks displays peaks associated with the partial attachment of the monolayer via a sulfonate moiety (see Table I) and confirms assignments in Figure 11. XPS was less sensitive to the presence of oxidized head groups that IR; longer exposures to atmosphere were required to confirm the products of oxidation by XPS. Similar changes are observed in the S(2p) spectra of alkanethiolate monolayers on silver although they occur at a slower rate.

the adsorbed thiolates to sulfonates.[29] The appearance of a strong peak at ~1200 cm^{-1} in the IR spectra of silver samples (Figure 11) is entirely consistent with a sulfonate head group.

Discussion

The data reported here support a general understanding of the structure of the alkanethiolate monolayers on copper, silver, and gold. The answer to the simplest question we can ask—"Are they the same?"—is clearly "no". How they differ is easily described in general terms.

Monolayers on Copper. All the evidence suggests that the films prepared on copper *under the conditions we used* (that is, by minimizing, but not completely excluding, exposure to laboratory atmosphere by manipulating the unfunctionalized metal under a flow of argon) can vary widely in character. The significant variations of spectral band intensities and line shapes all suggest that some factor related to the structure of the monolayer complicates this system. The clear inference from the XPS data is that the variations in the surface of the starting substrate, due to adventitious oxidation and other reactions with atmospheric constituents and, perhaps, to differences in the morphology of the surface, are likely underlying factors.

The copper surface that supports these monolayers is clearly not metallic. The O(1s) core level data establish that the copper contains oxygen. No Cu(II)($2p_{3/2}$) satellite structure could be detected by XPS; thus, the most likely phase present is a hydrous surface oxide related to Cu_2O. This oxide surface is also known to be highly active in the sorption of environmental contaminants as well as in the strong adsorption of CO_2 as carbonate. The microscopic topography of this surface is unclear. It is thus possible that any one or all of these factors could conspire to preclude the adsorption of thiols to the very high coverages or in the geometries necessary to form a structure comprised of close-packed and, perhaps, ordered alkyl chains. It is not surprising that copper samples prepared using apparently indistinguishable protocols yielded monolayers exhibiting various degrees of conformational disorder by IR and complementary differences in hysteresis of contact angles of water (see supplementary materials).

On clean elemental surfaces of Cu(111) under UHV conditions, simple thiols and disulfides (CH_3SH and CH_3SSCH_3) adsorb readily.[48] The surface species generated from either adsorbate is a surface thiolate, $CH_3SCu^{I}{\cdot}Cu^{0}{}_{n}$. The structure of this organic surface phase on Cu(111) has not yet been determined by LEED, but the evidence obtained from angle-resolved photoemission measurements supports a highly defined structural model containing a S–C bond projecting along the direction of the surface normal. Such a surface phase is qualitatively consistent with the character of the *best* monolayers we have prepared on copper although the values of α found suggest a somewhat different alignment of the all-trans chain ($\alpha \cong 12°$). In most instances, however, the data obtained in this study do not support a structure resembling the well-defined structure obtained in UHV. We therefore suggest that the oxide surfaces present in experiments involving adsorption from solution must seriously complicate the formation of dense organic phases. Under certain conditions this oxidation might be reversible and/or the Cu atoms removable as ions (Cu(+1)) to allow the formation of the dense phases seen on occasion. As noted, though, the experimental variable(s) involved remains undefined. Further oxidation of the surface after formation of the monolayer, and, possibly, oxidation of the thiolates as well, may also contribute to the disorder in the monolayer.[49]

The XPS data clearly suggest that the major sulfur species present is a thiolate (RSCu); the S(2p) core levels (Table I) are shifted by over 1 eV to lower binding energy from the position expected for a thiol (with the S–H bond intact). The same sort of species forms on elemental surfaces in UHV.[47] The microscopic morphology of the surfaces may be very different, and the influence on structure of surface sites occupied by oxide ions and by small quantities of alkyl sulfinic or sulfonic acids is presently unclear. The XPS data also strongly suggest that the bonding at the surface can be heterogeneous (a broad S(2p) envelope is sometimes seen). Whether this heterogeneity is attributable to different sulfur valence states or metal bonding sites is unclear.

Monolayers on Silver. In contrast to the copper-supported monolayer, the monolayers formed on silver are remarkably well-defined, and the assembly of monolayers on this metal better behaved than on copper. We would expect that silver, which also forms an oxide in air, might show complexities similar to those found for adsorption on copper. The core-level data clearly show, however, that nearly all of this oxide must have been removed on the adsorption of the alkanethiols and that oxidation subsequent to formation of the monolayer must be slow. We do not know at present where the residual oxygen detected by XPS remains, but suggest that grain boundaries are at least one likely candidate site. The data also show that this surface phase, when exposed to the atmosphere, gradually converts to what we believe is a material attached as a sulfonate; the O(1s) core level intensity seen at short immersions may, in fact, correspond to a partial surface coverage of this latter ligand. The signal-to-noise present in the XPS measurement makes the S(2p) core levels of this latter group hard to detect. The IR data require a structural model for fresh (not aged) monolayers on silver in which the chains are very densely packed. The line widths, the peak positions, and the shapes of the d^- and d^+ modes resemble those expected for a crystalline hydrocarbon solid to a remarkable extent. The structure we propose is thus one based on an all-trans chain with very few gauche conformations. The quality of the methyl band fits suggests that gauche conformations are probably less important in the phase diagram of these phases at 300 K than they are in the corresponding structures on gold (see below). The simulations in Figure 7 also define a structure in which the main chain axis

(48) Bao, S.; McConville, C. F.; Woodruff, D. P. *Surf. Sci.* **1987**, *187*, 133–143. Prince, N. P.; Seymour, D. L.; Woodruff, D. P.; Jones, R. G.; Walter, W. *Surf. Sci.* **1989**, *215*, 566–576.

(49) The bound thiolate and underlying copper surface each oxidize with extended exposure of the monolayer to atmosphere: Laibinis, P. E.; Whitesides, G. M. Unpublished results.

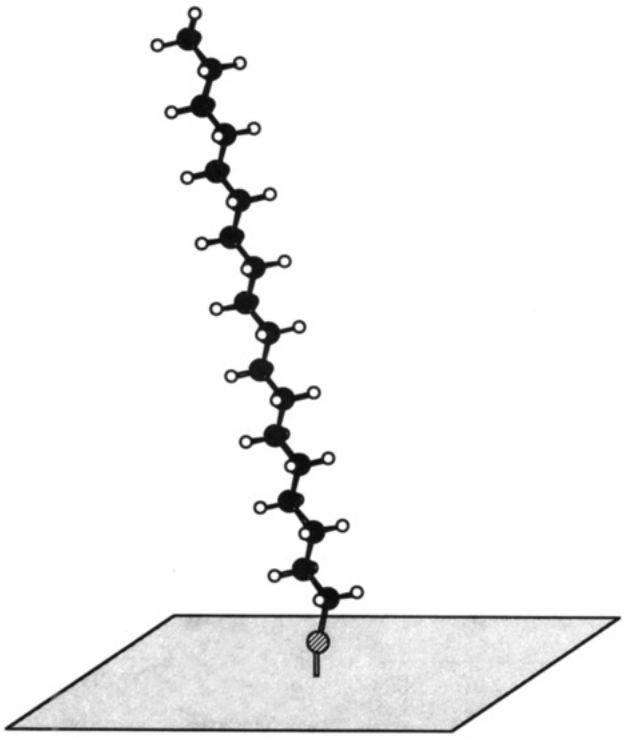

Figure 13. Space-filling model of an octadecanethiolate monolayer on silver as derived from infrared data interpreted in terms of a single-chain model.

is only very slightly canted from the surface normal direction. A graphical depiction of this structure is shown in Figure 13 for an octadecanethiolate monolayer. These results implicate a significant reduction of the interchain spacing in these phases in comparison to the analogous ones that have been extensively characterized on Au(111) in this and other papers. On this latter surface, we now know with great certainty that canted phases ($\alpha \cong 28°$ with the chain rotation $\beta \cong 52°$, see below) are formed whose character is well suited to the very strong tendency of this system to form ordered $(\sqrt{3} \times \sqrt{3})R30°$ sulfur overlayers. We believe that the canted surface phases seen on gold reflects the spacing of sulfur in this overlayer structure. The differing character of similar monolayers on silver, despite the similar metal–metal spacing for silver and gold, suggests that the same ordered overlayer is not formed on silver.[50]

Comparisons between Monolayers on Gold, Silver, and Copper. The differences in geometry (α and β) of the hydrocarbon portion of the assemblies on the coinage metal surfaces can be considered to arise from the balance of free energies from three sources: (1) the adsorbate/substrate interface, (2) the chain–chain packing of the interior of the assembly, and (3) the methyl interface (or solvent/methyl interface). The energetics of the first contribution above have been examined in the case of gold[30] (the energetics on silver and copper are no doubt similar) and are likely to be larger in magnitude than is possible from the energetics of hydrocarbon chain interactions[51] or hydrocarbon surface energies. Therefore, it is likely that head group/substrate energetics drive the major structural features of the entire assembly. After this consideration, one could ask the question of what structure of the hydrocarbon chain (tilt angle and packing) and what arrangement of surface methyl groups (orientation relative to the surface and to other methyl groups) represent minimum free energy structures given no constraint of surface/adsorbate bonding, viz., no preferred lattice spacing or valence angle. This question is impossible to answer experimentally at present, but, as judged by the infrared data, the two different classes of well-defined monolayers we observe (gold; silver and copper) both exhibit dense, crystalline packing, and in the case of gold, some compositional disordering at the air (or solvent) interface. The energy differences between these two classes of films, although indeterminate experimentally, may be as small as differences between orthorhombic and monoclinic phases of hydrocarbons.[44] Given this negligible difference and also given such a large discrepancy between the total free energies of the adsorbate/substrate interface and of the interior and the surface of the film for a particular system, it appears that the most likely factor determining the differences between two films formed on different substrates must be primarily the substrates themselves. On this basis, we consider the head group/substrate structure in detail first.

As has been noted, the XPS data indicate that the bonding to the surface is in the form of surface thiolates for the three metals. The literature contains considerable precedent for the bonding of sulfur-containing species on silver in this manner. On Ag(111) (the preferred crystallographic texture of the polycrystalline samples used in this study; see Experimental Section), elemental sulfur and H_2S have been found by LEED to form a number of stable, ordered surface phases.[52] The preferred habit is a $(\sqrt{7} \times \sqrt{7})R10.9°$ overlayer. This dense and structurally complex phase is believed to correspond to an ordered, lattice-matched interface between Ag(111) and (111)-oriented γ-Ag_2S. The silver in the first layer is believed to be ionic. Dimethyl disulfide dissociatively chemisorbs on Ag(111), and the surface thiolate formed also adopts the $(\sqrt{7} \times \sqrt{7})R10.9°$ structure.[53] The S–S nearest neighbor distance in such a structure is ~4.41 Å. It would thus seem that the bonding of sulfur in this sort of ionic surface phase (one that significantly reconstructs the (111) lattice plane) is consistent with the character of the phases inferred by infrared spectroscopy. Molecular dynamics calculations[54] suggest, however, that this lattice may be too dense (16.87 Å²/RS) to accommodate the all-trans chain sterically. The other phases seen in the H_2S adsorption studies,[52] most notably the $\sqrt{39}R16.1° \times \sqrt{39}\bar{R}16.1°$ overlayer (a structure corresponding to an ordered (100) layer of γ-Ag_2S), could also support the adsorption of the sulfur ligands at densities ~8% higher (~20.3 Å²/RS) than those in the $(\sqrt{3} \times \sqrt{3})R30°$ overlayers found on gold. The small angle of cant derived from IR data, we believe, reflects the short interchain spacings imposed by the silver/sulfur lattice. LEED or other

(50) Porter et al. have also characterized the structure and properties of *n*-alkanethiols adsorbed on evaporated silver films by wetting, ellipsometry, and IR (Walczak, M. M.; Chung, C.; Stole, S. M.; Widrig, C. A.; Porter, M. D. *J. Am. Chem. Soc.* **1991**, *113*, 2370–2378). A comparison with the results reported here for silver indicates general agreements between the sets of data, but shows differences for monolayers derived from shorter *n*-alkanethiols. For example, we do not observe an odd–even effect in the wettability of Ag/S-$(CH_2)_nCH_3$ by hexadecane (n = 4–8); Porter et al. do. They conclude that the hydrocarbon chain is canted at ~+13° *for all values of n*; we contend that the sign of the cant angle, α (Figure 6), alternates between positive and negative values for even and odd values of n, respectively. We believe their analysis to be in error. In both works, no variation in the intensities of methyl stretching modes was observed for $n \geq 5$. For shorter chain length (n = 4–7), Porter et al. observe as much as a 40% increase in the intensity of these modes. Our spectral simulations (Figure 7) suggest this variation is too small to be due to odd–even variations in chain length; we estimate that an ~100% increase in intensity is required. They conclude an odd–even effect is responsible for this variation but do not offer satisfactory explanation for its disappearance at $n \geq 8$. We rationalize this constant intensity by the existence of a single methyl orientation on silver as n is varied due to an alternation in the sign of the cant angle, α (Figure 14). Porter et al. also use corresponding odd–even variations in wettability for n = 4–8 (that we do not observe) as complementary evidence. We suspect most (if not all) of the differences between our work and that of Porter et al. to be due to adventitious (and perhaps contaminant promoted) oxidation of their evaporated films of silver prior to adsorption of the alkanethiol, and to the sensitivity of this system to surface oxidation when one uses shorter ($n \leq 6$) *n*-alkanethiols. We note that both papers have had difficulty preparing high-quality monolayers from shorter chain alkanethiols. We cannot, however, exclude some contribution to differences in the procedures used to prepare the silver films, and to resulting differences in grain size, preferred orientation, and surface topology.

(51) The group constituent heat of sublimation of normal hydrocarbons is 1.8 kcal/mol CH_2 at 0 K: Salem, L. *J. Chem. Phys.* **1962**, *37*, 2100–2113. For very long hydrocarbon tails ($n \gtrsim 20$), the enthalpies due to chain packing and the metal–head group interaction may well be of comparable magnitudes.

(52) Schwaha, K.; Spencer, N. D.; Lambert, R. M. *Surf. Sci.* **1979**, *81*, 273–284. Rovida, G.; Pratesi, F. *Surf. Sci.* **1981**, *104*, 609–624.

(53) Harris, A. L.; Rothberg, L.; Dhar, L.; Levinos, N. J.; Dubois, L. H. *Phys. Rev. Lett.* **1990**, *64*, 2086–2089. Harris, A. L.; Rothberg, L.; Dhar, L.; Levinos, N. J.; Dubois, L. H. *J. Chem. Phys.* **1991**, *94*, 2438–2448.

(54) Bareman, J. P.; Klein, M. L. *J. Phys. Chem.* **1990**, *94*, 5202–5205.

diffraction studies will be necessary to define the structure of this underlying lattice unambiguously.

Again, as is the case with copper, the *mechanism* of the adsorption of alkanethiol on silver is unclear. The oxidation of one or two monolayers of silver at the solid–air interface should be facile under the conditions used in the preparation of these samples. It is also clear from simple thermodynamic arguments both that an Ag(0) surface should be able to dissociate the S–H bond and that AgO_x species should be reducible by thiols. Given that metathetical replacements of oxygen atoms on some silver surfaces are also facile, it is easy to envision a number of processes leading to the materials seen experimentally. This latter chemistry also suggests another reason for the higher adsorbate densities which form on silver as compared to gold. The initial oxidation of the substrate by O_2 yields a high coverage of oxygen atoms on the surface.[17] Their substitution by sulfur would thus directly yield a surface phase of dense chains.[55] Even so, the precedent established by the UHV studies of dimethyl disulfide suggests that the formation of thiolates in high surface densities is intrinsic to the Ag(111) lattice plane.

As for both copper and silver, the bonding to gold also appears to be as a surface thiolate as judged by the core level shifts seen in the XPS data. The placement of the sulfur atoms in a $(\sqrt{3} \times \sqrt{3})R30°$ overlayer, as mentioned above, is now well established.[10,11] The picture we envision is one involving a more covalent structure than that on silver. On gold, there are no large displacements of the metal atoms from their normal (111) lattice sites. The constant chain cant angle seen in the gold system presumably reflects the dominant energetics of the metal–sulfur bond. The ordering seen reflects the interplay of the dominant energetic contributions of the metal–sulfur bonding and the second-order energetics of the packing of the alkyl chains. In the case of gold, the covalent character of the substrate bonding results in the adoption of a fixed Au–S–CH_2 valence angle, providing an interesting contrast to the behaviors seen on copper and silver.

Having discussed the dominant adsorbate/substrate interaction, we now turn to the issue of film structure. An intriguing point arising from the IR analysis is that the methyl mode spectra of the films formed on silver distinctly do not reflect changes in the absolute sign of the chain cant angle, α (Figure 6), with changing carbon chain length. If the absolute direction of the chain tilt were conserved with odd–even variation of length, the character of the spectra in the region of the methyl modes would vary considerably and be quite observable (see Figure 5). The presence of a disordered methyl surface, such as exists on gold, would diminish this effect somewhat, but the quality of the simulations in the region of the r^+ and r_b^- modes is sufficiently good (Figure 7) to indicate that gauche conformers are less important on silver than on gold. Using the conventions of orientation given in Figure 6, the chain structures on silver (and likewise on copper) are described in terms of ones in which *the chain is required to cant in opposite directions and the Ag–S–CH_2 valence angle to alternate between two different signs of α for odd and even numbers of methylene groups* (Figure 14). The methyl surface projection selected by each is the same dense phase, one which we can characterize as being more like a surface ethyl group (Figure 13) maximizing nearest neighbor interactions at the chain termini. Although the energetics associated with this methyl surface structure should be small, they seem to be sufficient to outweigh any preferences due to the sulfur. We believe this picture to be consistent with the hypothesis that the bonding of the sulfur at this surface is largely ionic.[53] With the above considerations in mind, we conclude that assembly of a given film proceeds so as to satisfy the adsorbate–substrate energetics first and then those associated with the methyl (ambient) surface (in the form of the ambient film surface tension).

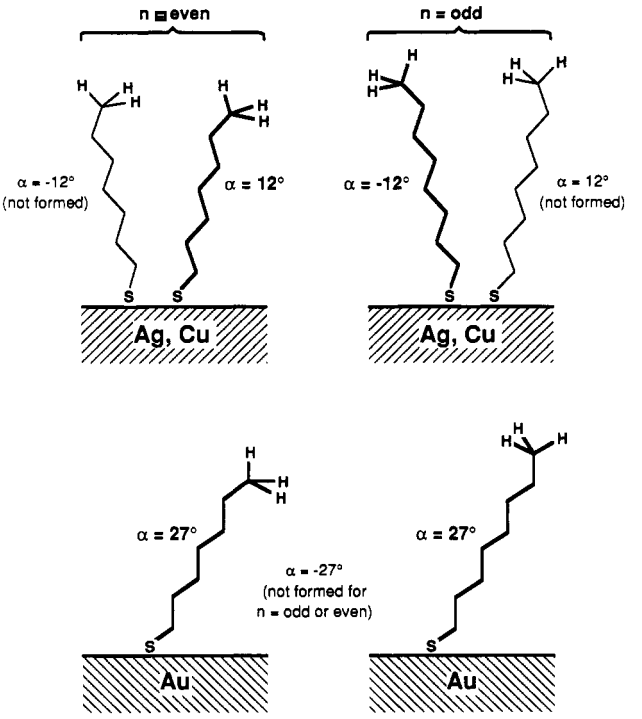

Figure 14. Illustration of the canted structures formed upon adsorption of *n*-alkanethiols, $CH_3(CH_2)_nSH$, on copper, silver, and gold. The structures that form on copper and silver do not exhibit any change in the intensities of methyl modes with incremental increase in the number of methylene groups (Figures 4 and 5). This observation is consistent only with the formation of a structure in which the cant angle, α, is positive for an even number of methylene groups and negative for an odd number of methylene groups; the geometry of the metal–thiolate interaction on these metals is not fixed as n is varied (upper panel). The structures formed on gold exhibit an odd–even modulation in the intensities of the methyl modes with increasing chain length (Figures 4 and 5). This modulation reflects the formation of a structure in which variations in the chain length of the adsorbate do not perturb the geometry of the gold–thiolate interaction (lower panel).

The structures formed on gold are understood quite consistently with the above principle. The placement of the sulfur atoms in a $(\sqrt{3} \times \sqrt{3})R30°$ overlayer with a fixed Au–S–CH_2 valence angle forces the chains into the same absolute orientation regardless of chain length. As a consequence, the orientation of the methyl group modulates with carbon number (Figure 5). There are, however, further subtleties to these structures. We also know, both from experiment and theory, that the lowest energy structure for this system does not involve a simple hexagonal lattice of the chains but, rather, is one reminiscent of the bimolecular monoclinic phases of the normal hydrocarbons.[56] We also know the symmetry of the methylene subcell cannot be simply orthorhombic as evidenced by the optical anisotropies in the infrared data (an orthorhombic subcell, at any value of α, would yield an average $\beta = 45°$[44] and be accompanied by d^+ and d^- intensity ratios approximately a factor of 2 different from those seen experimentally). To this point, both experiment and theory have failed to establish how important this two-chain unit cell is to the structure of the monolayer at temperatures greater than 220 K. The simulations presented in Figure 9 suggest that the structure present at 300 K may contain still significant signatures of this two-chain subcell. Our results also show that the IR data are consistent with, but do not independently establish, significant (perhaps as high as 45%) conformational disordering of the end

(55) See, for example: Wachs, I. E.; Madix, R. J. *Surf. Sci.* **1978**, *76*, 531–558. Sexton, B. A.; Madix, R. J. *Surf. Sci.* **1981**, *105*, 177–195. Stuve, E. M.; Madix, R. J.; Sexton, B. A. *Chem. Phys. Lett.* **1982**, *89*, 48–53. Stuve, E. M.; Madix, R. J.; Sexton, B. A. *Surf. Sci.* **1982**, *119*, 279–290. Canning, N. D. S.; Madix, R. J. *J. Phys. Chem.* **1984**, *88*, 2437–2446. Felter, T. E.; Weinberg, W. H.; Lastushkina, G. Y.; Zhdan, P. A.; Boreskov, G. K.; Hrbek, J. *Appl. Surf. Sci.* **1983**, *16*, 351–364. Au, C. T.; Singh-Bopari, S.; Roberts, M. W.; Joyner, R. W. *J. Chem. Soc., Faraday* **1983**, *79*, 1779–1791. Capote, A. J.; Madix, R. J. *Surf. Sci.* **1989**, *214*, 276–288; *J. Am. Chem. Soc.* **1989**, *111*, 3570–3577. Brainard, R. L.; Madix, R. J. *J. Am. Chem. Soc.* **1989**, *111*, 3826–3835 and references cited therein.

(56) Shearer, H. M. M.; Vand, U. *Acta Crystallogr.* **1956**, *9*, 379–384.

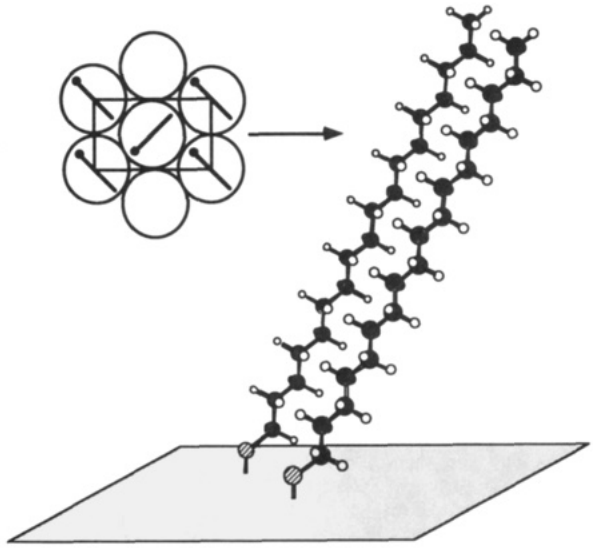

Figure 15. Illustration of the structure of a monolayer of an octadecanethiolate monolayer on gold inferred from a two-chain simulation based on all-trans chains. The inset shows the relationship of an orthorhombic chain sublattice (uncanted) relative to the hexagonal sulfur sublattice and the direction of the cant of the hydrocarbon chain for this arrangement as inferred from IR spectroscopy.

chain segments at 300 K. These "quantitative" values cannot be taken too literally, however, given the significant perturbations of the methyl group transition moments noted in the data. A schematic depiction of an idealized two-chain structure on gold is shown in Figure 15. The reader should note that this structure derives from only one fit to the data, howbeit one we believe to be plausible on the basis of steric arguments. Diffraction studies will be required to settle the importance of the two-chain unit cell at room temperature.

Structural Effects on Wetting. The structures on the three metals differ in significant ways that may affect their respective wettabilities. A significant issue that now exists for organized films is what are the detailed relationships between molecular features at surfaces, such as orientation and corrugation, and wetting. Wetting is influenced by a number of factors, among them molecular-scale and macroscopic roughness.[57] The monolayers we prepared on copper were of variable quality, in part due to morphological changes that occurred during oxidation and/or subsequent adsorption of the alkanethiol; monolayers on silver, in contrast, were more reproducible. Structurally, our highest quality monolayers prepared on copper were similar to monolayers prepared on silver. Given this similarity, we restrict our analysis to a contrasting of the structure–property relationships in wetting of monolayers formed on silver and gold.

The wettabilities of monolayers formed on silver and gold exhibit a common increase in hydro- and oleophobicity with increasing chain length (Figure 2). Similar progressions have been observed with alkanoic acids adsorbed on alumina.[37] The lower hydrophobicities of monolayers prepared from shorter alkanethiols ($n < 9$) have been rationalized previously in similar systems by assuming disordering of the shorter chain adsorbates and interaction of the probe liquid with the underlying metal substrate.[8,9,37] The limiting contact angles for monolayers derived from long ($n \geq 15$) alkanethiols are, within experimental error, the same on the three metals examined and are in accord with values reported for oriented alkyl monolayers on other substrates.[8,23-25] The films on silver, which we believe contain a smaller number of gauche conformers than those on gold, might be expected to present a lower energy interface expressing a more conformationally restricted and therefore homogeneous methyl surface. It seems most interesting, given these very different surface structures, that a difference in wettability is not observed.

It follows by inference from the lattice arguments above that the structures formed on gold can accommodate structural perturbations that are precluded on silver. The reconstruction of the methyl surface, whether driven thermally or in response to a contacting external phase, is affected mechanistically both by the population of gauche conformers and the unlocking of the chain tilt direction and magnitude.[42]

The canted structures on gold, in contrast to those formed on copper and silver, might presumably accommodate some partial intercalation of hexadecane by uncanting chain segments. The amount of void space generated by uncanting the hydrocarbon structure would be much greater on gold than silver; further, negligible space is probably available on silver since the chains are, prior to contact with a liquid, oriented near the surface normal ($\alpha \cong 12°$). Intercalation of hexadecane into a monolayer would result in a lowering of the advancing and receding contact angles of hexadecane and occur, based on structure, to the greatest extent possible on the materials formed on gold. The contact angles and hysteresis of hexadecane on the monolayers formed on silver and gold are, in fact, indistinguishable; we thus conclude that intercalation of hexadecane into monolayers on gold does not occur. Bain et al. found that alkanethiolate monolayers on gold prepared in hexadecane were not different (by ellipsometry, XPS, and wetting) from monolayers prepared from other solvents. This observation suggests that, even in the presence of a large excess of hexadecane, intercalation of solvent had not occurred.[20]

On gold, the orientation of the methyl groups at the monolayer–air interface is highly dependent on the number (odd versus even) of methylene groups in the adsorbate; monolayers on silver do not exhibit any orientational variation with chain length (Figure 5). The structural differences between these two monolayer systems allow comparison of an "odd–even" sensitive structure on gold with the "odd–even" neutral structure on silver as they relate to a surface-sensitive property, wetting. The wettabilities of water and hexadecane both monotonically increase with increasing chain length; no periodic trend is observed on gold (or silver). It is worthwhile to ask, in view of the magnitude of the differences in methyl orientation on gold, why there appears to be no influence on wetting. It is conceivable that the number of gauche conformers on gold, particularly in the region in contact with solvent, is sufficient to lessen the magnitude of the corrugation. There is, of course, no requirement that the structural characteristics of the monolayer when in contact with air (or vacuum) are preserved when the monolayer is placed in contact with a liquid. It is also entirely possible that hexadecane and water are sensitive to more than the ~0.5 Å that would be required to observe the small differences in structure that arise from conformational differences in the methyl groups.

In general, measurements of wetting on these interfaces were extremely useful in defining monolayers that were disordered or rough. They did not, however, allow discrimination between the two types of ordered structures observed here, even when the structures substantially affect (on the molecular level) the structure of the monolayer–vapor interface. Whatever differences exist between gold and silver in such structural details find little expression in wetting. Other probes of the structure of thin films (for example, helium diffraction[11]) may prove to be more sensitive to these sorts of perturbations.

Conclusions

n-Alkanethiols spontaneously assemble onto surfaces of copper, silver, and gold and form densely packed, oriented monolayer films. The films formed on silver and copper differ in structural detail from those formed on gold: the hydrocarbon chain is oriented more perpendicularly with respect to the surface; the films (when carefully prepared) exhibit a lower population of gauche conformations at room temperature; the orientation of the carbon–sulfur bond relative to the surface plane varies with chain length. The formation of reproducible films on copper and silver is com-

(57) Wenzel, R. N. *Ind. Eng. Chem.* **1936**, *28*, 988–994. Dettre, R. H.; Johnson, R. E. *Adv. Chem. Ser.* **1964**, *No. 43*, 136–144. Joanny, J. F.; de Gennes, P. G. *J. Chem. Phys.* **1984**, *81*, 552–562. De Gennes, P. G. *Rev. Mod. Phys.* **1985**, *57*, 827–863.

plicated by the sensitivity of these systems to exposure of the unfunctionalized or functionalized substrate to air, and to extended exposure to the solution containing the thiol. Films of high quality are, however, readily obtained with careful attention to detail. Extended exposure to alkanethiol solution results in reaction of the alkanethiol with the surfaces of silver and copper to form an interphase of metal sulfide on which an organized, oriented monolayer is supported. Although the systems of alkanethiols assembled on copper and silver are more difficult to work with than the corresponding systems on gold, this set of systems offers the opportunity to explore the effect of structural differences on a number of properties including wetting, intercalation, and capacitance.

Experimental Section

Materials. Materials were obtained from Aldrich and used as received unless specified below. Nonyl, undecyl (Pfaltz & Bauer), tetradecyl (Pfaltz & Bauer), and octadecyl thiols were distilled under reduced pressure prior to use. Heptadecyl, nonadecyl, and docosyl thiols were available from previous studies.[8,33] Pentadecanethiol was supplied by our colleague Kevin L. Prime (Harvard). Hexadecanesulfonic acid was obtained by acidification of sodium hexadecanesulfonate with sulfuric acid and purified by recrystallization from hexanes. Octadecanethiol-d_{37} was prepared from the corresponding perdeuterated bromide (Cambridge Isotopes, 98% D) by nucleophilic displacement by thioacetate and subsequent methanolysis with K_2CO_3/MeOH; the product exhibited TLC behavior identical with that of octadecanethiol and formed monolayers with indistinguishable properties (wetting, XPS, and ellipsometric thickness (for monolayers on gold)) from those formed from octadecanethiol. Solvents were obtained from Mallinckrodt and deoxygenated by bubbling N_2 for 30 min unless otherwise specified below or in the text; no further efforts were used to exclude air. Isooctane (Aldrich) was percolated twice through neutral alumina; ethanol (abs) was obtained from Quantum Chemical Corp. The silver and copper (Aldrich) and gold (Materials Research Corp.) used to prepare evaporated samples were of >99.99% purity. Silicon (100) wafers (100 mm) were obtained from Silicon Sense and washed with absolute ethanol. Prepurified Ar (>99.998%, <5 ppm O_2) was obtained from Med-tech.

Sample Preparation. Films of the various metals (1200–2000 Å) were prepared by evaporation subsequent to deposition of 200 Å of chromium or titanium (the latter being preferred) onto silicon wafers: evaporation of silver and copper were onto precut 1 × 3 cm^2 slides of silicon as well as onto silicon wafers; Au was evaporated onto silicon wafers and, in some cases, subsequently cut into slides. The evaporations were conducted in either a cryogenically pumped electron beam chamber (base pressure ~8 × 10^{-8} Torr), a cryogenically pumped resistive boat chamber (base pressure ~2 × 10^{-8} Torr), or a thermal evaporator evacuated with a diffusion pump (base pressure of <1 × 10^{-6} Torr); only monolayers prepared on copper were sensitive to the evaporator used. For evaporations of copper, the chamber was backfilled with prepurified argon immediately following evaporation (polyethylene bags were place around the openings of the evaporator to minimize diffusion of air into the chamber), and the substrates were transferred under a flow of argon to solutions in disposable scintillation vials. Films of silver were prepared either as described for copper or by backfill with N_2 and transfer of the substrates in air to solutions in Teflon containers. The backfill and transfer procedures typically took at the most 2 and 5 min, respectively.

Slides were removed from solutions after the stated duration of exposure, washed with absolute ethanol, blown dry with N_2, and characterized. Samples used for IR were prepared on 2-in. Si wafers and functionalized in Petri dishes.

The alkyl sulfonate samples were prepared by transferring freshly evaporated samples of copper and silver, in air, to solutions of hexadecanesulfonic acid (~1 mM) in isooctane. After ~12 h of immersion, the samples were washed with hexanes, blown dry with N_2, and characterized.

Morphology of the Substrate. The crystallographic textures of the highly reflective polycrystalline substrates supported on Si(100) used in this study were determined by X-ray diffraction. Two independent analyses were routinely made. The first (a so-called $\theta - 2\theta$ scan), involved the comparison of the intensities of an X-ray powder pattern to those of authentic powder sample. The second method, a somewhat simpler procedure, involved the determination of the (111) rocking curve for each substrate. Both copper and silver were found to be heavily (111) textured (although less so than gold). Copper depositions conducted under poor vacuum conditions yielded random polycrystalline surfaces. Characterization of the gold substrates has been reported previously.[36]

X-ray Photoelectron Spectroscopy (XPS). Spectra were obtained using a Surface Science SSX-100 X-ray photoelectron spectrometer that has previously been described.[33] High-resolution spectra were obtained at a pass energy of 50 eV using a 600-μm spot size; survey spectra (2 scans) were obtained at a pass energy of 100 eV and a 1000-μm spot size. Use of peaks associated with the underlying substrate as reference[58] [$Au(4f_{7/2})$ = 84.00 eV, $Ag(3d_{5/2})$ = 368.3 eV, $Cu(2p_{3/2})$ = 932.7 eV] leads to the unreasonable differences (range ≅ 0.6 eV) in the position of C(1s) associated with the monolayer which we believe were due to problems of calibration of our detector; spectra were instead referenced to C(1s) = 284.80 eV. Attenuation data were collected at a pressure of ~3 × 10^{-9} Torr and a pass energy of 100 eV using a 1000-μm spot size; the slides were characterized in random order by obtaining a single scan (~2 min) and fitting the resulting spectra with an 80% Gaussian/20% Lorentzian peak. Spectra of polycrystalline docosanethiol required use of a 2-eV flood gun to overcome charging; spectra were referenced to C(1s) = 284.80 eV.

Contact Angles. Static advancing and receding contact angles were measured on static drops using a Ramé-Hart goniometer under ambient conditions. Contacting liquids were applied (and removed) with a Matrix Technologies Electrapipette operated at its lowest speed (~1 μL/s). Contact angles were measured on both sides of the drop on at least 3 drops applied at different positions of the slide while the tip of the pipet remained attached.

Infrared Spectroscopy. The spectrometer, optics, and analytical protocols used in this paper have been described in earlier publications.[36,37,59] For the purposes of this study, given the difficulty of obtaining a clean reference spectrum on either silver or copper, we have used two different references: (1) monolayers prepared from octadecanethiol-d_{37} on the metal of interest as a reference mirror and (2) gold cleaned by oxidative treatment in either peroxysulfuric acid or ozone under UV irradiation (ABTECH). (*Caution: Peroxysulfuric acid reacts violently with organic materials and should be used with great care.*[60]) This procedure yields a spectrum for protonated samples in the 3000-cm^{-1} region whose intensities can be reliably used in the quantitative analysis from which the molecular orientations are deduced. All spectra are reported as $-\log R/R_0$ where R is the reflectivity of the substrate with the monolayer and R_0 is the reflectivity of the reference. Spectral simulations utilized film thicknesses determined for the most part by single wavelength ellipsometry. Several independent determinations were also made using spectroscopic ellipsometry over the wavelength 340–850 nm. The values used for calculations are as follows: (1) Au: C_{16} (19.0 Å), C_{17} (20.3 Å), C_{18} (21.6 Å), C_{19} (22.9 Å), C_{20} (24.0 Å), and C_{22} (25.5 Å); (2) Ag: C_{16} (21.5 Å), C_{17} (22.8 Å), C_{18} (24.1 Å), C_{19} (25.3 Å), and C_{20} (26.6 Å). We have noted earlier that ellipsometric studies of silver samples are somewhat problematic given the difficulty of obtaining reliable substrate constants. The values reported above were obtained from replicate measurements on substrates shielded from the laboratory ambient. The values selected were, as mentioned in the Results, from the lower range of experimental values, ones corresponding sensibly to the sizes of the adsorbate molecules used. None are larger than the all-trans extension of the chain. We believe these values to be accurate to within ~±1 Å. The worst projection of this error into calculations of the chain orientation is small (perhaps less than 2° in α on silver and gold). The most important point to note is that the numbers used are but one parameter used to simulate the optical anisotropies evidenced in the experimental data. Selection of thickness values corresponding to an all-trans extension of the chains would yield very similar quantitative fits to that shown above.

Note Added in Proof. Recent diffraction studies (X-ray and helium) have shown that the lattice constant of *n*-alkanethiolate monolayers supported on silver is shorter than that on gold. The unit cell of the former is ~10% less (nearest neighbor spacing of 4.77 Å), a result in very good agreement with that inferred from infrared spectroscopy. The overlayer formed is an incommensurate hexagonal phase, one reminiscent of an expanded $(\sqrt{7} \times \sqrt{7})R10.9°$ structure. See: Fenter, P.; Eisenberger, P.; Li, J.; Camillone, S., III; Bernasek, S.; Scoles, G.; Ramanarayanan, T. A.; Liang, K. S. *Langmuir*, in press.

The measured chain tilts on Au(111) are also found to be in good agreement with the values inferred from vibrational spectroscopy: G. Scoles (personal communication).

Registry No. HD, 544-76-3; Cu, 7440-50-8; Ag, 7440-22-4; An,

(58) Briggs, D.; Seah, M. P. *Practical Surface Analysis*; John Wiley: Chichester, 1983; Appendix 4 and references cited therein.
(59) Dubois, L. H.; Zegarski, B. R.; Nuzzo, R. G. *Proc. Natl. Acad. Sci. U.S.A.* **1987**, *84*, 4739–4742.
(60) Dobbs, D. A.; Bergman, R. G.; Theopold, K. H. *Chem. Eng. News* **1990**, *68* (17), 2. Erickson, C. V. *Chem. Eng. News* **1990**, *68* (32), 2.

7440-57-5; $CH_3(CH_2)_nSH$ (n = 3), 513-53-1; $CH_3(CH_2)_nSH$ (n = 4), 110-66-7; $CH_3(CH_2)_nSH$ (n = 5), 111-31-9; $CH_3(CH_2)_nSH$ (n = 6), 1639-09-4; $CH_3(CH_2)_nSH$ (n = 7), 111-88-6; $CH_3(CH_2)_nSH$ (n = 8), 1455-21-6; $CH_3(CH_2)_nSH$ (n = 9), 143-10-2; $CH_3(CH_2)_nSH$ (n = 10), 5332-52-5; $CH_3(CH_2)_nSH$ (n = 11), 112-55-0; $CH_3(CH_2)_nSH$ (n = 12), 19484-26-5; $CH_3(CH_2)_nSH$ (n = 13), 2079-95-0; $CH_3(CH_2)_nSH$ (n = 14), 25276-70-4; $CH_3(CH_2)_nSH$ (n = 15), 2917-26-2; $CH_3(CH_2)_nSH$ (n = 16), 53193-22-9; $CH_3(CH_2)_nSH$ (n = 17), 2885-00-9; $CH_3(CH_2)_nSH$ (n = 18), 53193-23-0; $CH_3(CH_2)_nSH$ (n = 19), 13373-97-2; $CH_3(CH_2)_nSH$ (n = 20), 66326-17-8; $CH_3(CH_2)_nSH$ (n = 21), 7773-83-3.

Supplementary Material Available: Table of wetting properties of monolayers prepared from different solvents, IR spectra of low-quality monolayers on copper, plot of intensity of CH_2 modes with chain length, and discussion of the methods used in simulating IR spectra (11 pages). Ordering information is given on any current masthead page.

Evaluating the Assumptions Underlying Force Field Development and Application Using Free Energy Conformational Maps for Nucleosides

David A. Pearlman† and Peter A. Kollman*

Contribution from the Department of Pharmaceutical Chemistry, University of California, San Francisco, California 94143-0446. *Received February 7, 1991*

Abstract: A recently developed method for applying constraints to internal coordinates during molecular dynamics is utilized to test a fundamental assumption in empirically based force field development: that it is acceptable to derive parameters by optimizing agreement between experiment and potential (rather than free) energy predictions. This new method is used in conjunction with free energy perturbation techniques to generate free energy contour maps in the γ-χ torsion plane for adenosine and deoxyadenosine nuclesides. These maps are compared with analogous potential energy maps, generated by using standard minimization techniques. While qualitatively similar, the maps display significant quantitative differences, calling into question the general validity of the fundamental assumption. The dependencies of the maps on the level of atomic representation (all atom versus united atom) and on the solvent model used (explicit versus implicit) are also examined. These comparisons make clear the large effects that even small changes in the representation can have. The calculations presented herein suggest that we can now advance to a new level of sophistication in our ability to incorporate experimental solvation and free energy results into force field development.

Introduction

The past two and a half decades have seen the rapid growth and evolution of a new field of chemistry: molecular modeling.[1,2] In molecular modeling, an empirically derived penalty ("energy") function is used in conjunction with various theoretical methods to predict molecular behavior.

Originally, this field was limited to molecular mechanics (minimization, systematic search) studies of small systems.[3] But subsequent leaps in computer power, coupled with algorithmic developments, have made possible more complex simulations. Among these recent advances are molecular dynamics (MD),[4,5] from which a dynamic picture of molecular behavior over time can be extracted, free energy perturbation (FEP),[6,7] which allows determination of the free energy difference between two states, and joint molecular dynamics-NMR or -X-ray refinement,[8,9] which provide a means to more efficient and reliable refinement of experimental data. These methods can be practically applied, in principal, to a broad range of systems, from small molecules to moderate-sized proteins.[10] Attempts have even been made to model systems as complex as membranes and ion channels.[11]

One feature common to all the aforementioned techniques is a reliance on a classical, primarily empirically based, potential energy force field (CPFF). Such a force field relates any system configuration to an analytically defined potential energy.[12] An example of a frequently used macromolecular CPFF that typifies those in use is[13,14]

$$V_{\text{Total}}(\mathbf{x}) = \sum_{\text{bonds}} K_r(r - r_{\text{eq}})^2 + \sum_{\text{angles}} K_\theta(\theta - \theta_{\text{eq}})^2 + \sum_{\text{dihedrals}} \frac{V_n}{2}[1 + \cos(n\phi - \gamma)] + \sum_{i<j} \left\{ \left[\frac{A_{ij}}{R_{ij}^{12}} - \frac{B_{ij}}{R_{ij}^{6}} \right] + q_i q_j / \epsilon R_{ij} \right\} + \sum_{\text{h-bonds}} \left\{ \frac{C_{ij}}{R_{ij}^{12}} - \frac{D_{ij}}{R_{ij}^{10}} \right\} \quad (1)$$

V_{Total} is the potential energy of the system, K_r and r_{eq} are the bond stretching constant and the equilibrium bond distance, K_θ and θ_{eq}

†Current address: Vertex Pharmaceuticals Incorporated, 40 Allston Street, Cambridge, MA 02139-4211.

(1) Kollman, P. *Annu. Rev. Phys. Chem.* **1987**, *38*, 303-316.
(2) Ramachandran, G. N.; Sasisekharan, V. *Adv. Prot. Chem.* **1968**, *23*, 283.
(3) Burkert, U.; Allinger, N. L. *Molecular Mechanics*; ACS Monograph Series; American Chemical Society: Washington, D.C., 1982; Vol. 177.
(4) McCammon, J. A.; Gelin, B.; Karplus, M. *Nature* **1976**, *267*, 585.
(5) van Gunsteren, W. F.; Berendsen, H. J. C. *Angew. Chem., Int. Ed. Engl.* **1990**, *29*, 992-1027.
(6) Postma, J. P. M.; Berendsen, H. J. C.; Haak, J. R. *Faraday Symp. Chem. Soc.* **1982**, *17*, 55-67.
(7) Tembe, B. L.; McCammon, J. A. *Comput. Chem.* **1984**, *8*, 281.
(8) Kaptein, R.; Zuiderweg, E. P. R.; Scheek, R. M.; Boelens, R.; van Gunsteren, W. F. *J. Mol. Biol.* **1985**, *182*, 179-182.
(9) Brunger, A. T.; Kuriyan, J.; Karplus, M. *Science* **1987**, *235*, 458-460.
(10) Allen, M. P.; Tildesley, D. J. *Computer Simulation of Liquids*; Oxford University Press: New York, 1987.
(11) McCammon, J. A.; Harvey, S. C. *Dynamics of Proteins and Nucleic Acids*; Cambridge University Press: New York, 1987.
(12) Rasmussen, K. In *Potential Energy Functions in Conformational Analysis*; Berthier, G., Dewar, M. J. S., Fischer, H., Fukui, K., Hall, G. G., Minze, J., Jaffe, H. H., Jortner, J., Kutzelnigg, W., Ruedenberg, K., Eds.; *Lecture Notes in Chemistry*; Springer-Verlag: New York, 1984; Vol. 37.

0002-7863/91/1513-7167$02.50/0